W-AM-Sym1 MOVING BACTERIAL FLAGELLA. Howard C. Berg, Department of Cellular and Developmental Biology, Harvard University, Cambridge, MA 02138.

Flagellated bacteria possess a remarkable motility system based on a reversible rotary motor linked by a flexible coupling to a helical propeller. The motor derives its energy from protons driven into the cell by gradients or electrical fields. Its direction of rotation depends, in part, on signals processed by sensory systems. I will tell you how I think this motor works.

W-AM-Sym2 DNA IN SLOW MOTION. Charles Cantor, Columbia Univ., Coll. of P&S, NYC 10032.

W-AM-Sym3 MACROMOLECULAR MOTION IN THE CYTOSKELETON. Thomas D. Pollard. Department of Cell Biology and Anatomy, Johns Hopkins Medical School, Baltimore, MD 21205.

The cytoskeleton is a paradoxical structure. It is rigid enough to resist compressive and tensile deformations and elastic enough to recover from small deformations. It is also plastic enough to tolerate complete transformations of cellular shape over the period of minutes to hours. At the same time, two of its major components, actin filaments and microtubules form tracks for organelle movements and cables to transmit tension from place to place in the cell.

An important feature of this complex structure is that many of its constituent protein subunits bind to each other relatively weakly. This introduces a critical temporal element into many of the molecular interactions. The resulting high frequency molecular rearrangements may be responsible for many of the paradoxical properties of the whole system. For example, networks of actin filaments and the crosslinking protein alpha-actinin are very stiff when deformed rapidly and indistinguishable from actin alone when deformed slowly, because the alpha-actinin binds to and dissociates from the filaments rapidly, perhaps 20 times per second. When the network is stressed rapidly, it resists displacement of the filaments, but when the network is stressed slowly, the crosslinks can rearrange faster than the filaments are displaced.

I will review how weak, rapid interactions between proteins participate in the assembly of actin filaments and microtubules, the crosslinking of the cytoskeletal polymers and the production of the forces that cause bulk contraction and organelle movement.

W-AM-Sym4 DIFFUSION IN REDUCED DIMENSIONS: FACILITATED LOCATION OF DNA TARGET SITES BY REGULATORY PROTEINS. Peter H. von Hippel and Otto G. Berg*. Institute of Molecular Biology, University of Oregon, Eugene, OR 97403, U.S.A. (*Present Address: Dept. of Molecular Biology, The Biomedical Center, Box 590, S-75124 Uppsala, Sweden.)

A number of proteins that regulate gene expression can be shown, in in vitro experiments, to locate their specific DNA binding targets at rates that appear to be appreciably faster than diffusion-controlled. This indicates that target location does not proceed entirely by three-dimensional diffusion, but must involve facilitating processes of reduced dimensionality; i.e., diffusion or transport of the protein to the target site while nonspecifically bound to other regions of the DNA. Available evidence for the existence of such processes in a number of systems will be reviewed, and proposed mechanisms of both the transport process and the ultimate recognition of the specific target site will be discussed. Mechanisms of analogous facilitated diffusion processes in membrane-receptor and enzyme-substrate interactions will also be considered. (Supported by USPHS Research Grants GM-15792 and GM-29158 and the Swedish Natural Science Research Council.)

W-AM-A1 AMINO ACID SEQUENCE OF A SUBFRAGMENT-2 PEPTIDE IN TURKEY GIZZARD MYOSIN HEAVY CHAIN. Gabor Huszar, Lynne Vigue and *Marshall Elzinga, Dept. Ob/Gyn, Yale Univ. School Medicine, New Haven, Conn. 06510 and *Brookhaven National Laboratories, Upton NY 11973.

As a part of our studies on the isozymic differences among myosins in smooth muscles, we have isolated and determined the N-terminal amino acid sequence of a peptide arising from the turkey gizzard myosin heavy chain. The myosin heavy chain purified by Sepharose-4B chromatography was cleaved with CNBR and the digest was subjected to isoelectric focusing. The peptide was isolated from the gel by urea extraction and differential solubilization. The primary structure of 40 amino acid residues was determined by automated amino acid sequencing with the following results: -Arg-Gln-Lys-(His)-Thr-Gln-Ala-Val-Glu-Glu-Leu-Thr-Glu-Gln-Leu-Glu-Gln-Phe-(Lys)-(Lys)-(Ala)-(Lys)-Ala-Asn-Leu-Asp-Lys-Thr-Lys-Gln-(Thr)-Leu-(Glu)-Lys-Asp-Asn-Ala-Asp-(Ser)-Gln-. Comparing the amino acid sequence with the available information on the primary structure of myosin heavy chains from other sources, we have established that this peptide in turkey gizzard myosin is homologous (50% identical) to that of the subfragment-2 segment in nematode myosin. The amino acid sequence has also shown homology to the corresponding myosin region in rabbit skeletal muscle (13 residues identical): in fact, it arises from the part of subfragment-2 which was identified as the putative hinge region by Lu and Wong (JBC, 260:3456, 1985). At present, we are attempting to isolate homologous CNBR peptides in other smooth muscle sources to further study the isozymic differences among myosin heavy chains previously demonstrated by the two dimensional isoelectric focusing/SDS peptide gel patterns.

W-AM-A2 IDENTIFICATION OF THE TWO PHOSPHORYLATION SITES FOR PROTEIN KINASE C ON THE 20,000 DALTON LIGHT CHAIN OF SMOOTH MUSCLE MYOSIN. Mitsuo Ikebe, Marshall Elzinga*, and David J. Hartshorne**. Dept. of Physiol. and Biophys., Case Western Reserve Univ.* Dept. of Biol. Brookhaven Natl. Lab. **Dept. of Biochem. and Nutrition and Food Sci. Univ. of Arizona.

Phosphorylation of gizzard heavy meromyosin (HMM) by protein kinase C was studied. Gizzard HMM was phosphorylated 4 mol of P/mol of HMM by protein kinase C. All phosphorylation sites were located at 20,000 dalton light chain judged by autoradiogram of SDS gel and Urea gel electrophoresis. Rate of phosphorylation for the first phosphorylation site was 6 times faster than that for the second site. Phosphorylated gizzard HMM was subjected to acid hydrolysis and electrophoresis to determine the phospho amino acid. At a phosphorylation level of below 2mol of P/mol of HMM, most of the phosphoamino acid was threonine, whereas phospho serine was also observed at a phosphorylation level of more than 2mol of P/mol of HMM. The doubly phosphorylated 20,000 dalton light chain was hydrolyzed with trypsin and phosphorylated peptides were isolated by reverse phase chromatography. Following amino acid analysis and sequence determinations it was found that the phosphorylation sites were threonine 9 and serine 2 or 1. Therefore, it was concluded that the first phosphorylation site is threonine 9 and that the second phosphorylation site is serine 2 or serine 1. Dephosphorylation of these sites with gizzard phosphatase and aorta phosphatase was also measured. Two sites were dephosphorylated at a same rate by gizzard phosphatase, although the rate of dephosphorylation was 2.5 times slower than that for serine 19 (phosphorylation site by myosin light chain kinase). Aorta phosphatase dephosphorylated only threonine 9 and the rate of the dephosphorylation was 11 times slower than that for serine 19. Supported by NIH grants AR38431 to M.I. and HL23615 and HL20984 to D.J.H., and by American Heart Association, North Ohio Affiliate to M.I.

W-AM-A3 PROTEOLYTIC FRAGMENTATION OF CHICKEN GIZZARD CALDESMON. Sumitra Nag, Yude Qian, C.-L. Albert Wang and John C. Seidel, Dept. of Muscle Research, Boston Biomedical Research Institute, Boston, MA 02114

We have studied the structure of chicken gizzard caldesmon (CaD) by various proteolytic enzymes. Treatment of CaD with chymotrypsin or papain results in formation of intermediate fragments that are relatively resistant to further proteolytic digestion. No specific cleavage sites were apparent on digestion of CaD by trypsin. Chymotryptic digestion initially produces two major bands on SDS gel electrophoresis migrating at 80 and 40 kDa. Subsequent digestion of the 80 kDa fragment by chymotrypsin leads to formation of peptides corresponding to 54 kDa and 29 kDa, whereas the disappearance of the 40 kDa fragment is accompanied by the appearance of multiple bands with molecular weight of about 18 kDa. Among these chymotryptic fragments we found that the 40 kDa fragment retained calmodulin- and F-actin-binding properties and inhibition of actomyosin ATPase activity, in agreement with a report of Szpacenko and Dabrowska (FEBS Lett. 202, 182, 1986). Digestion with papain produces two major fragments with molecular weights of 41 kDa and 16 kDa; neither of these fragments binds to calmodulin or F-actin. When the chymotryptic digestion mixture containing 80, 54 and 40 kDa fragments was subjected to papain cleavage, the same (41 kDa and 16 kDa) fragments were obtained, suggesting that the 41 kDa papain fragment is derived from the 80 kDa chymotryptic fragment, and arises from a different region of the CaD molecule than does the 40 kDa chymotryptic fragment. Supported by grants from NIH, MDA and AHA.

W-AM-A4 THIN FILAMENT-LINKED REGULATION IN VERTEBRATE SMOOTH MUSCLE. Michael P. Walsh, Gisele C. Scott-Woo, Megan S. Lim, Cindy Sutherland and Philip K. Ngai, Department of Medical Biochemistry, University of Calgary, Calgary, Alberta, Canada T2N 4N1.

The possibility of thin filament-linked regulation of vertebrate smooth muscle contraction has been investigated by application of the myosin competition test to chicken gizzard actomyosin, and isolation and functional characterization of native thin filaments of chicken gizzard. Hybridization of gizzard actin and associated proteins (present in crude actomyosin preparations) with rabbit skeletal muscle myosin resulted in an actin-activated myosin Mg^{2+}-ATPase activity which exhibited 50.3 ± 4.1% (n = 6) Ca^{2+}-sensitivity. On the other hand, no Ca^{2+}-sensitivity was observed when purified gizzard actin and tropomyosin were hybridized with skeletal myosin. Chicken gizzard thin filaments consisted almost exclusively of actin, tropomyosin, caldesmon and an unidentified 32 kilodalton polypeptide. When reconstituted with phosphorylated gizzard myosin, these thin filaments conferred Ca^{2+}-sensitivity (67.8 ± 2.1%; n = 5) on the myosin Mg^{2+}-ATPase. On the other hand, no Ca^{2+}-sensitivity of the myosin Mg^{2+}-ATPase was observed when purified gizzard actin or actin plus tropomyosin was reconstituted with phosphorylated gizzard myosin. Native thin filaments were rendered essentially free of caldesmon and the 32 kilodalton polypeptide by extraction with 25 mM $MgCl_2$. When reconstituted with phosphorylated gizzard myosin, caldesmon-free thin filaments and native thin filaments exhibited the same Ca^{2+}-sensitivity. The observed Ca^{2+}-sensitivity, therefore, is not due to caldesmon but is due to calmodulin and/or an unidentified minor protein component of the thin filaments which may be an actin-binding protein involved in regulating actin filament structure in a Ca^{2+}-dependent manner.

W-AM-A5 ISOMYOSINS IN VASCULAR SMOOTH MUSCLE. Anne F. Martin, Ellen G. McMahon, and David C. Robinson. Univ. of Cinn. Coll. of Med., Cinn., OH 45267-0575.

We examined the isomyosin composition in adult and 12 day old rat, rabbit and dog abdominal aorta by electrophoresis on non-denaturing polyacrylamide gels. Two isomyosins of approximately equal density were apparent in rabbit and dog aorta. We designated the protein with the fastest mobility SMM-1 and that with the slower mobility SMM-2. Adult rat aorta contained one predominant (SMM-1) isoform with a second minor component (SMM-2). There was an increase in SMM-2 relative to SMM-1 in aorta from 12 day old rats. SMM-1 and SMM-2 are not phosphorylated species of a single isomyosin. No change in the relative proportions of SMM-1 and SMM-2 was observed in phosphatase treated actomyosin from rat aorta. However, phosphorylation of actomyosin with [γ^{32}P]ATP increased the mobility of the SMM-1 myosin relative to the non-phosphorylated control. Since SMM-2 constitutes less than 10% of the myosin population, changes in this component were difficult to detect. When phosphorylated actomyosin was co-electrophoresed with actomyosin prepared by our usual procedure, a third band with a greater mobility than SMM-1 was apparent and 90% of the counts were present in this band. We have shown that myosin is present in both bands designated SMM-1 and SMM-2 using antibodies to tracheal and platelet myosins. The antibody to tracheal myosin reacted strongly with SMM-1 and very slightly with SMM-2 transblotted onto nitrocellulose. The antibody to platelet myosin reacted with both SMM-1 and SMM-2. The myosin in long term cultures of smooth muscle cells from rat aorta co-electrophoresed with SMM-2 and reacted with antibody to platelet myosin on immunoblots. Our data suggests that SMM-2 is a developmental form of smooth muscle myosin and that isomyosin expression in vascular smooth muscle is developmentally regulated as in striated muscle.

W-AM-A6 TWO SMOOTH MUSCLE MYOSIN HEAVY CHAINS DIFFER IN THEIR LMM FRAGMENT. T.J. Eddinger and R.A. Murphy. Dept. of Physiology, School of Medicine, Univ. of Virginia, Charlottesville, VA 22908.

Two different forms of the myosin heavy chain (SM1 and SM2) exist in equal amounts in many smooth muscles. They may combine to form a single obligatory heterodimer in native smooth muscle myosin, rather than combining randomly to form three isozymes (Rovner et al. Am. J. Physiol. 250: C861-870, 1986). The aim of this study was to determine the structural difference between SM1 and SM2. Purified swine stomach myosin, or extracts from stomach and carotid all showed a single native myosin band on 4% pyrophosphate gels when the myosin was dephosphorylated. Activation of swine carotid media tissues produced myosin phosphorylation and three distinct bands could be resolved on pyrophosphate gels containing non-, mono-, and di-phosphorylated myosin. No evidence for isozymes was obtained by this approach. The same samples show two distinct bands on SDS gels with apparent MW's of approximately 210 (SM1) and 205 kD (SM2). Peptide maps of SM1 and SM2 differed. Heavy meromyosin and subfragment-1 from SM1 and SM2 both had the same mobility on SDS gels; while a doublet or series of doublets differing in mobility was obtained for light meromyosin (LMM). Each band of the LMM doublet (approx. 100 and 95 kD) was cut out of a 10% SDS gel for peptide mapping. Different peptide patterns were observed for LMM-SM1 and LMM-SM2. A monoclonal antibody produced against swine stomach myosin bound equally to SM1, SM2, LMM-SM1 and LMM-SM2 on western blots of SDS gels. Varying digestion conditions allowed clipping of the carboxyl terminal of these fragments and eliminated antibody recognition. We conclude that a difference peptide(s) of 3-5 kD is located in the LMM region of SM1 and SM2. This difference is not at the carboxyl terminal recognized by the monoclonal antibody. Supported by USPHS Grant 5 PO1 HL 19242 and the Am. Heart Assoc., VA Affiliate

W-AM-A7 IDENTIFICATION OF A VARIANT OF THE 17,000 DALTON MYOSIN LIGHT CHAIN IN VASCULAR SMOOTH MUSCLE. David R. Hathaway, Debra J. Helper and Joseph A. Lash. Department of Medicine, Krannert Institute of Cardiology, Indiana University School of Medicine, Indianapolis, IN 46202

Smooth muscle myosin consists of two heavy chains (M_r=200,000) and two dissimilar sets of light chains (M_r=20,000 and 17,000). While the 20,000 dalton (LC_{20}) light chain appears to be involved in a phosphorylation-dephosphorylation reaction that can regulate the actin-activated ATPase activity of smooth muscle myosin, the precise function of the 17,000 dalton light chain (LC_{17}) is not known. Recently, we have identified two forms of LC_{17} in bovine aortic smooth muscle. These forms, LC_{17a} and LC_{17b}, can be separated by isoelectric focusing (IEF) of purified myosin or by two dimensional electrophoresis (i.e. IEF/SDS-PAGE) of muscle homogenates. LC_{17b} is more negatively charged (pI=4.5) than LC $_{17a}$ (pI=4.6). Approximately 65% of LC_{17} is present as LC_{17b} and 35% as LC_{17a} in aortic muscle. In contrast, more than 95% of LC_{17} identified by IEF/SDS-PAGE of porcine stomach and bovine tracheal smooth muscle is present as LC_{17b}. Moreover, only a single species of LC_{17} (pI=4.52) is observed in chicken gizzard smooth muscle. Although antibodies raised against total bovine aortic LC_{17} strongly cross react with gizzard LC_{17}, reverse phase HPLC of tryptic digests suggests that aortic LC_{17} is structurally different from gizzard LC_{17} and aortic LC_{17a} and LC_{17b} also possess unique peptide differences. In conclusion, our studies suggest that bovine aortic myosin is heterogeneous, containing species with LC_{17} isoforms. This finding provides another potential mechanism for regulation and diversity of actin-myosin interaction in smooth muscle.

W-AM-A8 ACTIN-ACTIVATION OF VASCULAR SMOOTH MUSCLE MYOSIN: EFFECTS OF MYOSIN LIGHT CHAIN PHOSPHORYLATION, TROPOMYOSIN AND CALDESMON. David R. Hathaway, Department of Medicine, Krannert Institute of Cardiology, I.U. School of Medicine, Indianapolis, IN 46223.

<u>In vitro</u> measurements of the actin-activated ATPase activity of vascular smooth muscle myosin may be modulated by a number of factors including phosphorylation of the 20,000 dalton light chain (LC_{20}), the presence of tropomyosin, divalent cations, filamentous state of myosin and caldemson. Recently, we have confirmed the findings of Wagner (J. Biol. Chem. 261:7778, 1986) and have found that phosphorylation of the 20,000 dalton light chains of vascular smooth muscle myosin is not required for full actin-activated ATPase activity. Myosin was purified from bovine aortic smooth muscle and found to contain approximately 0.1 mol PO_4/mol LC_{20}. It could be phosphorylated to 1.0 mol PO_4/mol LC_{20} using ATPγS and purified myosin kinase. Both native (UP-MYO) and thiophosphorylated (P-MYO) myosins could be actin-activated: UP-MYO, V_{max}=40 nmol/min/mg, Kapp=150 uM; P-MYO, V_{max}=50 nmol/min/mg, Kapp=12 uM. Inclusion of chicken gizzard tropomyosin (ratio to actin 1:5) decreased Kapp for actin and increased V_{max} values: UP-MYO, V_{max}=98 nmol/min/mg, Kapp=80 uM; P-MYO, V_{max}=105 nmol/min/mg, Kap=5.2 uM. Irrespective of the state of myosin LC_{20} phosphorylation or the presence or absence of tropomyosin, caldesmon was a potent inhibitor of actin-activated ATPase activity, fully suppressing activity at a molar ratio to actin of 1:5. These results suggest that phosphorylation of purified vascular smooth muscle myosin <u>in vitro</u> predominantly affects the Kapp for actin-activated ATPase activity. While tropomyosin enhances V_{max} and reduces Kapp it is not required for actin-activation of UP-MYO. Finally, caldesmon is an effective inhibitor of actin-activated ATPase activity whether myosin is phosphorylated or not.

W-AM-A9 REGULATION OF PLATELET MYOSIN. James R. Sellers and Estelle V. Harvey, NHLBI, LMC, Bethesda, MD 20892.

In order to understand the role of light chain phosphorylation in the regulation of the MgATPase activity of a cytoplasmic myosin, the effect of actin on the MgATPase activity of phosphorylated and unphosphorylated myosin from human platelets has been studied in 50 mM KCl, 10 mM $MgCl_2$, 0.1 mM EGTA, 0.5 mM DTT, 10 mM imidazole (pH 7.0). The results indicate that phosphorylated myosin has a 6-10-fold higher V_{max} than does unphosphorylated myosin (0.56 s^{-1} vs. 0.046 s^{-1}, respectively for the average of 5 experiments). The K_{app} is decreased less than 4-fold by phosphorylation (9.4 μM vs. 34.4 μM for phosphorylated and dephosphorylated myosin, respectively). In these experiments the phosphorylated myosin is usually greater than 85% phosphorylated whereas the unphosphorylated myosin is usually less than 10%. It should be emphasized that these experiments have been carried out with intact myosin as opposed to heavy meromyosin (HMM), since it has been difficult to prepare an intact, regulated HMM from platelets. The large effect of phosphorylation on V_{max} is similar to previous findings with turkey gizzard smooth muscle HMM (Sellers <u>et al.</u>, J. Biol. Chem. <u>257</u>, 13880, 1982) and is in contrast to recent data reported by Wagner and George (Biochem. <u>25</u>, 913, 1986) for myosin from bovine thymus where the effect of phosphorylation is a large decrease in K_{app} with little effect on V_{max}.

W-AM-A10 REGULATION OF ACANTHAMOEBA MYOSIN I BY HEAVY CHAIN PHOSPHORYLATION: UNCOUPLING THE REGULATORY AND CATALYTIC SITES BY TRYPTIC DIGESTION. Thomas J. Lynch, Hanna Brzeska and Edward D. Korn, Laboratory of Cell Biology, National Heart, Lung, and Blood Institute, NIH, Bethesda, MD

Heavy chain phosphorylation is required for maximal actin-activation of the Mg^{2+}-ATPase activities of myosins IA and IB. Phosphorylation increases the V_{max} rather than decreasing the K_{ATPase}, but details of the regulatory mechanism are not known. Limited chymotryptic digestion of myosin IA produces a fully active NH_2-terminal 100-kDa fragment: phosphorylation increases its actin-activated Mg^{2+}-ATPase 30- to 40-fold and also its affinity for actin (e.g. 5-fold in the absence of nucleotide). Further tryptic digestion produces an NH_2-terminal 38-kDa fragment which contains the nucleotide-binding site and a 74-kDa fragment which includes the phosphorylation site. Under nondenaturing conditions, these peptides remain associated with each other and the undigested light chain in a complex which retains full EDTA-ATPase activity, binds F-actin with higher affinity in the absence of ATP than in its presence, and can be maximally phosphorylated (1 mole/mole) at apparently the correct site by heavy chain kinase. However, this phosphorylation has no effect on the catalytic or actin-binding properties of the complex. Specifically, the actin-activated Mg^{2+}-ATPase and affinities for actin of the 38/74 complex, whether phosphorylated or not, are virtually identical to those of the unphosphorylated 100-kDa fragment. These results indicate that the phosphorylation site of the 38/74 complex is uncoupled from the catalytic and actin-binding sites and that the integrity of the heavy chain in the region of the 38/74 junction is required for full activation of myosin IA by heavy chain phosphorylation.

W-AM-A11 THE MOLECULAR MECHANICS OF ACANTHAMOEBA MYOSIN II FILAMENT FORMATION. Mark A.L. Atkinson, Sybren S. Wijmenga, Blair Bowers and Edward D. Korn, LCB, NHLBI, and LCP, NIADDK, NIH, Bethesda, MD 20892.

The actin-activated Mg^{2+}-ATPase activity of myosin II from Acanthamoeba castellanii is regulated cooperatively at the level of the myosin filament by the phosphorylation of 3 serines close to the C-terminus of each heavy chain. To elucidate the molecular mechanics of this regulation, we have analyzed the intermediates in the polymerization of myosin II into bipolar filaments by analytical ultracentrifugation, transient electric birefringence and electron microscopy. We propose that the tails of myosin II monomers in solution are not straight but that a hinge exists about 345 Å from the C-terminus. The monomers form side-by-side parallel dimers with their heads staggered by 300 Å. The C-terminal 66 amino acids, which include the phosphorylation sites, are important in the antiparallel interactions which are essential for the formation of bipolar filaments from dimers. We propose a self-limiting assembly model for the formation of myosin II filaments which produces a structure containing 16 monomers with adjacent heads staggered by 150 Å. In this model of the filament, phosphorylation/dephosphorylation could regulate enzyme activity via either a transition in the secondary structure of the terminal, non-helical 26 amino acids, which would affect filament packing or conformation, or by interactions between the phosphorylation sites and the putative hinge region. In either case, structural changes in the filament dependent on the phosphorylation state could affect the flexibility of the hinge, and hence the mobility of the head which contains the active sites, and thus regulate enzyme activity.

W-AM-A12 COMPLETE NUCLEOTIDE SEQUENCE AND DEDUCED POLYPEPTIDE SEQUENCE OF A NON-MUSCLE MYOSIN HEAVY CHAIN GENE: EVIDENCE OF A HINGE IN THE ROD-LIKE TAIL. J.A. Hammer III, B. Bowers, B.M. Paterson, and E.D. Korn, LCB, NHLBI, and LB, NCI, NIH, Bethesda, MD 20892.

Acanthamoeba myosin II (MII) is a non-muscle myosin possessing conventional myosin structure. MII is phosphorylated/dephosphorylated within a small C-terminal non-helical tailpiece which shifts MII between enzymatically inactive and active forms, probably by altering the conformation of the small MII bipolar filaments. We have sequenced a 6 kilobase region of Acanthamoeba genomic DNA which contains an entire MII heavy chain gene. The gene encodes a 1509-residue heavy chain polypeptide. Three small introns interrupt the protein coding sequence; the positions of two of these introns are exactly conserved relative to several muscle myosin genes. The MII globular head amino acid sequence shows a high degree of similarity with the sequences of vertebrate and invertebrate muscle myosins. By contrast, there is no compelling and unique way to align the MII rod-like tail sequence with that of muscle myosins. However, the chemical nature of the MII tail sequence, i.e. the periodicity of hydrophobic and charged residues, is typical of muscle myosins. Analysis of the MII tail sequence and electron microscopy of MII molecules reveal the existence of a hinge where the rod-like tail can bend sharply. We conclude that MII and muscle myosins diverged from a common ancestral gene and that the tolerance for sequence divergence in the rod-like tail domain is considerable as long as the chemical nature of the sequence necessary to form the αhelical coiled-coil structure and to stabilize filament assembly is maintained. We speculate that the hinge may play a key role in the molecular mechanism by which phosphorylation of the non-helical tailpiece alters filament conformation and, consequently, ATPase activity.

W-AM-B1 MODULATION OF GATING AND CONDUCTANCE PROPERTIES OF INACTIVATING K CHANNELS IN GH3 CELLS. P. Kay Wagoner and G.S. Oxford. (Intr. by C. Wm. Davis) Department of Physiology, University of North Carolina, Chapel Hill, NC 27514.

Currents associated with inactivating K channels were recorded in GH_3 cells using the patch voltage clamp technique. Conductance through these channels is modulated by the type of monovalent or divalent cations bathing the membrane. Outward conductance is increased as external K^+ is elevated. Internal Cs^+ produces a voltage-dependent block at an effective electrical distance of 1.08. This block is relieved by elevating external K^+. These observations are consistent with multi-ion properties and can be fit by a 3B2S rate theory model. External Co^{++} and Cd^{++} (but not Mg^{++} or organic Ca^{++} channel blockers) reduce peak outward current and shift the inactivation-voltage curve in the depolarizing direction. Inactivation is dramatically altered by group-specific protein reagents. Internal but not external SITS (200uM-1mM) slows the rate of inactivation and increases peak currents without affecting the steady-state inactivation-voltage curve. External or internal NBA (1uM to 1mM) decreases the rate of inactivation, increases peak current and prevents complete inactivation of 30% of the conductance by potentials greater than -10mV. The peak effect of internal NBA occurs at 4 minutes while that of external NBA is present in 15 seconds. Complete recovery of normal inactivation follows brief exposure to low (10uM) concentrations of NBA. Longer applications or higher concentrations lead to irreversible effects on inactivation. Neither internal nor external TNBS effects inactivation of these currents. Divalent cations and group-specific reagents may provide useful tools for the study of inactivating K channels. (Supported by NIH grant NS18788).

W-AM-B2 CALCIUM AND POTASSIUM IONS ALTER THE RATE OF POTASSIUM CHANNEL INACTIVATION IN T LYMPHOCYTES. Stephan Grissmer and Michael Cahalan, Department of Physiology and Biophysics, University of California, Irvine Ca 92717.

We investigated the kinetics of K^+ channel inactivation in the human T-cell-derived cell line Jurkat E6-1 using the patch-clamp whole-cell recording technique. The pipette solution contained in mM: 160 K aspartate, 1.1 EGTA, 0.1 $CaCl_2$, 2 $MgCl_2$ and 5 HEPES. Increasing extracellular $[Ca^{2+}]_o$ from $< 10^{-8}$ M (1 mM EGTA, no added Ca^{2+}) to 106 mM speeds the rate of inactivation during a pulse to +40 mV by a factor of about 5. The inactivation time constant, τ_h, determined by fitting a single exponential to the decay of the K^+ current was 361 ± 23 ms (mean ± S.D.; n=6) in 0 Ca^{++}, 278 ± 26 ms (n=44) in normal Ringer with 2 mM Ca^{2+}, and 74 ± 23 ms (n=3) in 106 mM Ca^{2+}. In contrast, increasing $[K^+]_o$ from 0 to 160 mM, holding $[Ca^{2+}]_o$ constant at 2 mM, reduced the rate of inactivation. The decay of the K^+ current in high $[K^+]_o$ was well fitted by a double exponential with fast and slow inactivation time constants, τ_{hf} and τ_{hs}. τ_{hf} values were similar to τ_h in normal Ringer, whereas τ_{hs} was on the order of 4 to 10 s, a slow inactivation not seen in normal Ringer. The observations can be explained by assuming that the rate of inactivation is enhanced when Ca^{2+} binds to a site, with a binding constant of approximately 1.4 mM. K^+ either competes with Ca^{2+} for this site or prevent Ca^{2+} from reaching this site. Increasing the intracellular Ca^{2+}-buffering by including 55 mM BAPTA and 5 mM Ca^{2+} in the pipette did not change the effect of Ca^{2+} on τ_{hf}, suggesting that this Ca^{2+} binding site is not located at the cytoplasmic surface of the K^+ channel. Supported by a DFG fellowship Gr 848/2-1 (S.G.) and by NIH grants NS14609 and AI21808.

W-AM-B3 UNUSUAL INACTIVATION OF POTASSIUM CURRENT (I_K) IN CELL BODIES OF THE GIANT AXONS IN 'GULF' SQUID. F.T. Horrigan, M. Lucero, H.-T. Leung, T. Brismar and W.F. Gilly, Hopkins Marine Station of Stanford University, Pacific Grove, CA 93950.

Loliguncula brevis is a small squid found in warm, inshore waters of the Texas-Louisiana Gulf coast. Cell bodies in the giant fiber lobe (GFL) of the stellate ganglion give rise to giant axons in the same way as in Loligo sp. Axon-less cell bodies were enzymatically isolated from excised GFL tips and maintained in primary culture (15°C) for no more than 3 days before study using a whole cell voltage clamp technique. I_K in Loliguncula cell bodies is very similar in several respects to I_K in giant axons of Loligo: 1) Voltage dependence and kinetics of activation, 2) Differential sensitivities of channel opening and closing kinetics to Zn and Mn ions, 3) Properties of outward I_K block by aminopyridines, 4) Properties of inward I_K block by external Cs ions.

Inactivation of I_K in GFL cells is complex and markedly different from that in axons. First, pronounced 'cummulative' inactivation occurs following a large, brief pulse and greatly reduces I_K during a subsequent depolarization. This process develops with the time course of channel closing after the first pulse and recovers over several hundred ms at 12°C. Second, two components of inactivation of outward I_K are apparent during a large depolarization with time constants of approximately 100 ms vs. 15 ms at 12°C. Recovery from both processes is slow. The proportion of rapidly inactivating I_K increases dramatically with temperature above 18-20°C. Living Gulf squid are extremely tolerant of water temperature, provided it remains higher than this level; below this they display severe behavioral disorders and quickly die (time constant of several minutes; recovery nonexistant). I_K in GFL cells from Loligo opalescens have nearly identical properties in all regards, but these cold-water squids are sensitive to water temperature in the opposite way. We acknowledge Marine Biomedical Institute, Univ. Texas, Galveston for squid.

W-AM-B4 INACTIVATION OF A-CHANNELS IN NEONATAL RAT NODOSE NEURONS. A. Shrier and E. Cooper. Department of Physiology, McGill Univ., Montreal, Quebec, Canada H3G 1Y6 (Intr. by D.E. Goldman).

The A-current is a transient outward potassium current found in a wide variety of cells. Previously we described the inactivation of the A-current from nodose neurons at the single channel level (J. Physiol. 386: 199-208, 1985) and found that for voltage steps to positive potentials activation was rapid and inactivation was due to mean channel open time. The present study was undertaken to learn more about the inactivation of these channels. Using a two step protocol, we can demonstrate directly that A-channels can proceed from the closed state to the inactivated state without opening. Furthermore, our results indicate that the extent of inactivation affects only the probability of channel opening and does not influence the latency for channel activation, mean channel open time or single channel conductance. In addition, although most A-channels open and close directly to the inactivated state in tens of msecs, we sometimes find that in a series of voltage steps to a given level, A-channels can appear that open and close repeatedly for hundreds of msecs before closing to the inactivated state. This gating behaviour can persist for a number of consecutive steps. It is tempting to speculate that an intracellular factor(s) can shift the A-channel between the short inactivation and the long inactivation, and thereby provide a mechanism for modulation of the A-current.

Supported by the Medical Research Council of Canada.

W-AM-B5 DELAYED RECTIFICATION IN HEART CELLS: SINGLE CHANNEL AND WHOLE CELL CURRENTS. K.B. Walsh, J.P. Arena and R.S. Kass. University of Rochester, Department of Physiology, 601 Elmwood Avenue, Rochester, NY 14642.

We report measurement of delayed rectifier K^+ channel currents in enzymatically-dispersed rat and guinea pig ventricular cells. Whole cell inward rectifier currents (IK_1) were measured from 120 mV to + 100 mV and leak currents were determined by addition of $BaCl_2$. Outward IK_1 could be measured up to 50 mV positive to V_K. At voltages positive to this, no time-independent current could be detected through this channel. Delayed rectifier currents (I_K) were identified in whole cell recordings by a time-dependence that became evident only at voltages more positive than -10 mV. The I/V for I_K showed rectification in the inward direction, but not as strongly as IK_1. In 4.8 mM K_o, cell-attached single channel records revealed the existence of at least three distinct K channels at voltages near +50 mV (resting potential +120 mV) that could be distinguished by their unitary amplitudes and kinetics. A large amplitude current (3 pA) was eliminated in excised patches exposed to ATP (2 mm)-containing solutions. An intermediate amplitude current (1.5 pA) was seen in rat, but not guinea pig cells. Its ensemble averaged record resembles the early outward transient reported in whole cell studies of these cells. Finally, a small amplitude current (0.5 pA) was observed in both rat and guinea pig cells. Activity of this channel could be seen in both cell attached and excised patches. The ensemble average for this current showed a time dependence very similar to that of the whole cell recordings of guinea pig I_K. These results strongly suggest that the low amplitude single channel currents reflect activity of I_K channels.

W-AM-B6 INWARD RECTIFICATION OF HEART POTASSIUM CHANNEL (K1) DEPENDS ON INTERNAL MAGNESIUM. Carol A. Vandenberg, Dept. of Physiology, UCLA, Los Angeles, CA 90024.

The inward rectifier (K1) from isolated adult guinea pig ventricular cells was studied to examine the mechanism of rectification. Voltage ramps of single channels in cell-attached patches produced I-V relationships that rectify strongly with a sharp bend at a potential near E_k when $[K]_{out}$ was varied from 25-230 mM. No outward current could be detected. Identical rectification was observed in excised patches, or in cell-attached patches in which the cell was permeabilized with saponin (MgATP was included in the intracellular solution to inhibit the K_{ATP} channel). The rectification point also paralleled E_k when $[K]_{in}$ was changed. Rectification could be eliminated by excision of the patch into a solution containing ATP without Mg, and it could be restored by the addition of 1 mM free Mg to the internal solution. In low Mg solutions (< 100 μM), intermediate degrees of rectification were obtained, and the current at potentials positive to E_k was often interrupted by brief closures. The kinetics of this process are being examined with noise analysis of single channels. These studies suggest that rectification of K1 may be due to internal block by Mg, possibly the result of rapid block of the open channel.

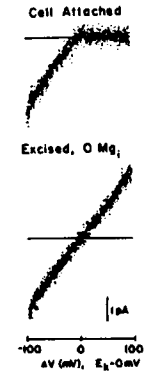

W-AM-B7 BLOCK BY Ba^{2+}, Sr^{2+}, Ca^{2+} OF Cs^+, Rb^+, AND K^+ CURRENTS THROUGH THE INWARDLY RECTIFYING K^+ CHANNEL IN ISOLATED GUINEA PIG VENTRICULAR MYOCYTES: IMPLICATIONS ON CHANNEL GATING. Raman Mitra and Martin Morad, Dept. of Physiology, University of PA, Philadelphia, PA 19104.

Cesium ions are considered fairly impermeant through K^+ channels; however, it was possible to record time and voltage-dependent inward Cs^+ currents through the inwardly rectifying K^+ channel in the presence of only Cs^+ and Ca^{2+} in the external solution and N-methyl-d-glucamine as the only internal cation. Cs^+ currents were observed only if the holding potential was > -50 mV or by preceding the test pulse with a depolarizing prepulse. Cs^+ currents activated near -10 mV but showed no inactivation up to -20 mV. More negative test pulses increased the peak current, the rate of activation and inactivation and decreased the steady state current. Removing external Ca^{2+} completely suppressed the inactivation of the Cs^+ current, while increasing the Ca^{2+} increased the rate and magnitude of inactivation at all potentials. Equimolar substitution of Cs^+ by Rb^+ yielded similar results but the currents were about 8-10 fold greater. With K^+ no inactivation of the current was observed except at very negative potentials (< -100 mV). Ba^{2+} and Sr^{2+}, like Ca^{2+}, blocked the monovalent currents in a time and voltage dependent manner but were more potent. By considering the effect of the membrane electric field on the concentration of a cation at a binding site within the channel one can explain the data by the following affinity sequence for the site: $Ba^{2+} > Sr^{2+} > K^+ > Rb^+ \geq Ca^{2+} > Cs^+$. This binding sequence is the same found for a highly K^+ selective synthetic ligand, cryptate 222 (Lehn & Sauvage, 1975, J. Am. Chem. Soc. 97:6700), whose binding rate constants with mono- and divalent cations are consistent with the time constants of activation and inactivation that we measured for the inwardly rectifying K^+ channel, suggesting that channel 'gating' may represent the kinetics of ion binding to a site within the channel.

W-AM-B8 PHARMACOLOGICAL DISSECTION OF TWO HEART K CHANNELS: THE INWARD RECTIFIER AND THE DELAYED RECTIFIER. J.P. Arena and R.S. Kass. University of Rochester, Department of Physiology, 601 Elmwood Avenue, Rochester, NY 14642.

We report the differential block of inward rectifier (IK_1) and delayed rectifier (IK) K channel currents by two externally applied quaternary ammonium (QA) derivatives Clofilium and LY 97241. K channel currents were recorded at room temperature from enzymatically isolated guinea pig ventricular cells using a whole cell arrangement of the patch clamp technique. Pipette solutions contained ATP (3 mM) and EGTA (11 mM) to eliminate ATP- and Ca-activated K channel currents. Cells were held at zero current potentials and brief (40 msec) voltage pulses were applied in the absence and presence of $BaCl_2$ (1-5 mM) to determine the IK_1 instantaneous current/voltage relationship (I/V) and leak currents. Longer pulses (1-2 sec) were used to study IK. We find that the (QA) compound Clofilium ((4-chloro-N.N-diethyl-N-heptyl) benzene butaminium) is highly selective for IK. Clofilium (50-100 uM) reduces IK 50-70% with little or no effect on IK_1. In contrast, a closely related structural analog, LY 97241 (N-ethyl-N-heptyl-4-nitrobenzenebutanimine) applied at similar concentrations blocked 90% of both IK and IK_1. Block was not observed if the compounds were applied internally. We tested for, but found little evidence of, voltage-dependent block and competition with extracellular K. Our results suggest that both of these channels can be blocked by externally accessible QA derivatives, the receptors for these drugs are not within the membrane field, and that slight structural modifications can selectively block one or both of these channels.

W-AM-B9 MODULATION OF DELAYED RECTIFIER POTASSIUM CHANNELS BY cAMP IN FROG SKELETAL MUSCLE. J. Arreola and J.A. Sánchez. Department of Pharmacology, CINVESTAV-IPN. Ap. Postal 14-740, Mexico, D.F., 07000.

In a previous work we showed that Epinephrine and cAMP modulate calcium channels in frog skeletal muscle (Biophys. J. 49, 197a, 1986). The present experiments show that delayed rectifier potassium channels are also modulated by cAMP.

Vaseline-gap, voltage-clamp experiments were performed (Rana montezumae). Control solutions: external (mM). Mg^{2+}=10, TMA^+=106, $CH_3SO_3^-$=131.6, K^+=5.6, TTX=30×10^{-7}, MOPS=4, pH=7.2. Internal: EGTA=77, K^+=154, MOPS=4, $MgCl_2$=1.5, ATP(Na_2)=2, pH=7.1. cAMP (1mM) was added to the cut ends and fibers were incubated for 25-30 minutes. A 1 min. interval was allowed between records.

cAMP increased I_K (mean ± S.E., (n)) by 46.2±13.2% (5) at -40 mV. Tail current experiments showed a linear instantaneous I-V relation in both cases. Maximum g_K increased by 54.8±6.7% (4).

No major kinetics effects were observed: the currents could be superimposed by a scale factor except for long despolarizing pulses (250 ms) where the time constant of decay decreased significantly by cAMP which suggests a change in E_K.

In line with the cAMP experiments, intracellular recordings in intact fibers revealed a slight effect of Epinephrine (10^{-6}M) in the (dV/dt)min of action potentials from -88.6±4.3 V/s (9) to -94.6±2.0 V/s (7) without any effect on resting potentials (-91.5±0.5 mV (9) and -91.2±0.7 mV (7)).
Supported by CONACYT PCCBNA-022593 and J. Ricardo Zevada grants.

W-AM-B10

WITHDRAWN.

W-AM-B11 **TWO TYPES OF POTASSIUM CHANNELS IN RAT TYPE II ALVEOLAR EPITHELIAL CELLS: DIFFERENTIAL SENSITIVITY TO THE FLUORESCENT DYE PHOSPHINE 3R.** Thomas E. DeCoursey and Elizabeth R. Jacobs. Departments of Physiology & Medicine, Rush Medical College, Chicago, IL 60612.

Type II alveolar epithelial cells secrete surfactant, which prevents lung collapse by reducing surface tension. Using gigohm-seal recording, we have studied type II cells isolated from rats and maintained in primary culture We previously reported delayed rectifier potassium channels in rat type II cells (Jacobs et al, *Am. Rev. Resp. Dis.* 133:A89). When using a fluorescent dye, phosphine 3R, to identify individual voltage-clamped type II cells, we frequently **(but not exclusively)** see a different type of K channel, also activated upon depolarization, but at more positive potentials, with higher TEA (tetraethylammonium) sensitivity ($Ki \simeq 100$ μM), faster tail currents, and faster recovery from inactivation. Both K channel types appear identical to those described in mouse T lymphocytes (DeCoursey, Chandy, Gupta & Cahalan, *J. Gen. Physiol.*, in press, April, 1987). The more frequent observation of highly TEA-sensitive K channels in phosphine-identified cells may reflect differential sensitivity to the dye. Both types of K currents are reduced reversibly by addition of phosphine to the bath, but delayed rectifier channels are more sensitive. Phosphine also reversibly shifts K channel activation to more positive potentials. When phosphine-stained cells are excited to fluoresce ($\lambda \simeq$ 420-485 nm), delayed rectifier currents are irreversibly reduced, this effect being dependent upon the duration of the excitation. The TEA-sensitive K currents appear less affected. The effects of phosphine 3R constrain its use for identifying type II cells, but facilitate study of highly TEA-sensitive K channels.

W-AM-B12 A VOLTAGE-DEPENDENT POTASSIUM CONDUCTANCE IN AVIAN HEPATOCYTES Carla Marchetti and Arthur M. Brown - Department of Physiology and Molecular Biophysics, Baylor College of Medicine, Houston, Texas 77030.

Voltage-dependent ion channels may play an important role in the regulation of liver membrane potential and hormone driven functions. Whole-cell and single channel outward currents were studied with the patch recording technique in dissociated hepatocytes from newborn chicks. In an external bath containing (mM) 135 NaCl, 5.4KCl and 1.8 $CaCl_2$ and with a pipette solution containing 140 mM KCl, currents activated at -15 mV, had a sigmoidal time course of activation, which could be fitted by n^2 kinetics, and no inactivativation in 500 ms. The maximum outward conductance was 6.6 ± 2.4 nS in 18 cells. The reversal potential shifted of 49.5 mV per ten fold increase in external potassium concentration, indicating that the current was mainly carried by K ions. The current was reversibly blocked by 5mM 4-aminopyridine. $BaCl_2$ (2 mM) caused an inhibition of 78% from a holding potential of -50 mV and of 93% from -80 mV, at +10 mV. The current was not dependent on either external or internal (10^{-5} - 10^{-9} M) Ca concentration. Single channel recording in ouside-out patches revealed single channels with a unitary conductance of 6 pS and bursting kinetics. The mean open time was 12.81±0.18 ms and mean closed times 1.57±0.37 ms and 16.31±1.91 ms (3 patches). All these observations are consistent with the interpretation of the potassium channel in chick hepatocytes as a voltage-dependent delayed rectifier.

W-AM-C1 CHARACTERISTICS OF [^{3}H]-RYANODINE BINDING TO SOLUBILIZED VESICLES FROM OVINE CARDIAC SARCOPLASMIC RETICULUM

Zachary I. Hodes, Samuel H. Boyer, IV, and Eduardo Marban. Department of Medicine and The Howard Hughes Medical Institute, The Johns Hopkins University, Baltimore, MD 21205

Calcium release from the SR plays a central role in excitation-contraction coupling in adult mammalian heart. Ryanodine, a compound which blocks Ca release from the SR, exhibits specific binding (in its tritiated form) to solubilized microsomes of skeletal muscle (Pessah et al, J. Biol. Chem., 1986). We have extended this work to ovine cardiac microsomes, as the first step towards purifying the ryanodine binding site. Microsomes were solubilized at a concentration of 5 mg protein/ml in 5 mg/ml CHAPS, 1M NaCl, 40mM Tris-maleate, pH 7.1, 10μM PMSF. [^{3}H]-ryanodine binding was characterized in the pellet obtained by centrifugation at 110,000 x g in a 100 μL volume of 0.1% CHAPS, 0.5M NaCl, 40mM Tris-maleate, pH 7.1, 300μM $CaCl_2$ with [^{3}H]-ryanodine at concentrations of 0.5-100nM (final protein concentration = 500μg/ml). Samples were incubated with shaking at 37°C for 80 min. Assays were collected on Whatman GF/C filter paper pre-soaked in 5% polyethylenimine, rinsed 3 times with ice-cold deionized water, and counted in non-aqueous scintillant. Solubilization of 100 mg protein yielded 40 mg of protein in the pellet. Specific binding to this fraction, utilizing 100μM unlabeled ryanodine as blank, indicates a single high-affinity site of K_d = 3.7nM and B_{max} = 0.8 pmol/mg protein, with 80-90% specific binding. The non-hydrolyzable ATP analog AMP-PCP (5 mM) does not significantly alter binding characteristics in our solubilized preparation. These results indicate the existence of high-affinity ryanodine binding sites in solubilized cardiac SR.

W-AM-C2 IMMUNOPRECIPITATION OF [^{3}H]RYANODINE RECEPTOR FROM RABBIT SKELETAL MUSCLE SARCOPLASMIC RETICULUM.

C. Michael Knudson, Toshiaki Imagawa, Albert T. Leung, Steven D. Kahl, John Sutko and Kevin P. Campbell. Dept. of Physiology and Biophysics, University of Iowa, Iowa City, IA 52242 and Dept. of Pharmacology, University of Nevada, Reno, NV 89557.

A monoclonal antibody capable of immunoprecipitating [^{3}H]ryanodine receptor from solubilized skeletal muscle triads has been produced. BALB/C mice were immunized with isolated triads enriched in the ryanodine receptor. Hybridoma supernatants were screened for anti-ryanodine receptor antibodies using an immunoprecipation assay with solubilized [^{3}H]ryanodine-labelled receptor. [^{3}H]Ryanodine labeled triads were solubilized in digitonin and incubated with goat-anti-mouse IgG beads that had been previously incubated with monoclonal antibodies from ascites fluid or culture media. [^{3}H]Ryanodine binding activity in the void was determined using a polyethylene glycol precipitation assay and correlated inversely with the activity precipitated with the beads. Monoclonal antibody XA7 precipitated [^{3}H]ryanodine binding activity from the prelabeled solubilized triads and this antibody stained a protein with a relative molecular mass of 350,000 Da on immunoblots. The 350,000 Da protein was absent from light sarcoplasmic reticulum vesicles (which are devoid of [^{3}H]ryanodine binding) and enriched in isolated triads. Binding of [^{3}H]ryanodine to the immunoprecipitated receptor was stimulated by mM ATP and inhibited by μM ruthenium red. Our results strongly suggest that the 350,000 Da protein of the junctional sarcoplasmic reticulum is the ryanodine receptor and possibly a component of the Ca^{2+} release channel. The effects of monoclonal antibody XA7 on Ca^{2+} release from the sarcoplasmic reticulum vesicles is currently being determined. (Supported by NSF 85-17834 and MDA).

W-AM-C3 PURIFICATION OF THE RYANODINE RECEPTOR (RyR) AND IDENTITY WITH FEET STRUCTURES OF JUNCTIONAL TERMINAL CISTERNAE (JTC) OF SARCOPLASMIC RETICULUM (SR)

Makoto Inui, Akitsugu Saito, Sidney Fleischer, Dept. of Molecular Biology, Vanderbilt Univ., Nashville, TN 37235

The RyR has been purified from JTC of SR from fast skeletal muscle. The RyR was solubilized with CHAPS. The solubilized receptor showed the same [^{3}H]-ryanodine binding properties as the original SR vesicles in terms of binding characteristics. Purification of the RyR was performed by a combination of column chromatography in the presence of CHAPS. The purified RyR bound 393 ± 65 pmol ryanodine per mg protein (mean ± S.E., n=5). The purified RyR showed three bands on SDS-PAGE with M_r of 360K, 330K and 175K. Densitometry indicates that these are present in a molar ratio of 2/1/1, suggesting a monomer ic unit with a M_r of 1.225 x 10^6 and supported by gel exclusion chromatography in CHAPS. Electron microscopy of the purified and reconstituted RyR shows the square shape of 210 Å characteristic of and comparable in size and shape to the feet structures of JTC of SR, indicating that ryanodine binds directly to the feet structures. From the ryanodine binding data, the stoichiometry of ryanodine binding sites to feet structures is estimated to be about 2. Since the RyR is coupled to Ca^{2+} gating, the present finding suggests that the RyR and Ca^{2+} release channel represent a functional unit, the structural unit being the foot structure which, *in situ*, is junctionally associated with the transverse tubules (TT). It is across this triad junction that the signal for Ca^{2+} release is expressed. Thus, the foot structure appears to directly respond to the signal from TT, causing release of Ca^{2+} from the junctional face membrane of the JTC of SR. (Supported by NIH AM 14632 and Muscular Dystrophy Assoc. to S.F. and Investigatorship of American Heart Association, Tennessee Affiliate to M.I.)

W-AM-C4 ISOLATION OF THE JUNCTIONAL FEET-RYANODINE RECEPTOR COMPLEX FROM CARDIAC AND SKELETAL SARCOPLASMIC RETICULUM. F. ANTHONY LAI, JULIA S. HENDERSON and GERHARD MEISSNER (Intr. by C. CARTER) Departments of Biochemistry and Physiology, University of North Carolina, Chapel Hill, NC 27514

Ryanodine, a neutral plant alkaloid, has been shown to interact specifically, and with high affinity to the Ca^{2+} release channel of sarcoplasmic reticulum (SR). We now report that the high molecular weight (HMW) junctional feet proteins comigrate with the ryanodine binding protein upon sucrose density gradient centrifugation. A "heavy" canine cardiac and rabbit skeletal SR vesicle preparation with enriched Ca^{2+} release activity was labelled with [^{3}H]ryanodine, solubilized in a CHAPS detergent medium, and the extract centrifuged through a linear sucrose gradient. A single peak of specific ryanodine binding activity was observed with apparent sedimentation coefficient of 30 S for skeletal and 33 S for cardiac SR. Pretreatment of extract with DTT did not affect the sedimentation profile, whereas heating destroyed all specific ryanodine binding. Ryanodine binding and SDS-PAGE analysis of gradient fractions indicated a similar specific enrichment (20-50X) in the 30 and 33 S peaks of the ryanodine receptor, the HMW feet proteins (M_r 320,000 and 290,000), and two bands of M_r 160,000 and 260,000. This suggests that the SR Ca^{2+} release channel protein and the HMW feet proteins are both present in a large oligomeric complex comprising subunits of M_r 160,000-320,000. The lack of ryanodine binding proteins of lower S value and presence of feet proteins only in the peak of ryanodine binding also suggests that the latter have either a specific anchoring function for the Ca^{2+} release channel, or be otherwise involved in the Ca^{2+} release process. Supported by NIH grants AM 18687 and HL 27430.

W-AM-C5 PHTHALOYCANINE DYES INDUCE RAPID CALCIUM EFFLUX FROM SARCOPLASMIC RETICULUM VESICLES BY AN OXIDATION REACTION. Jonathan J. Abramson, Joseph R. Cronin, Guy Salama*. Portland State University, Department of Physics, P.O. Box 751, Portland, OR 97207 and *Department of Physiology, University of Pittsburgh, Pittsburgh, PA 15261.

The copper containing phthalocyanine dyes, alcian blue, copper phthalocyanine tetrasulfonic acid, and Luxol fast blue MBSN cause rapid Ca^{2+} efflux from actively loaded SR vesicles. At 5μM Alcian blue, with 1mM free Mg^{2+}, a Ca^{2+} efflux rate of ∿10 n moles/mg/sec is observed. Ca^{2+} efflux is inhibited by ruthenium red, and high external Mg^{2+} concentrations, and is stimulated by adenine containing nucleotides. Preincubation of alcian blue with the reducing agents, sodium dithionite, dithioerythreitol or a large excess of cysteine caused a dramatic inhibition of Ca^{2+} release from SR. Reoxidation of the alcian blue leads to a return of Ca^{2+} release activity. Copper phthalocyanines are structurally similar to metalloporphyrins. They appear to be causing Ca^{2+} release from SR vesicles by oxidizing a group associated with the Ca^{2+} release channel from sarcoplasmic reticulum. Supported by AHA, Alaska, Oregon and Western Penn. Affiliates of AHA, and PHS RO1-NS18590. J.A. is an established Investigator of AHA, G.S. is supported by RCDA-NS00909.

W-AM-C6 OXIDATION OF THE CALCIUM RELEASE PROTEIN FROM SARCOPLASMIC RETICULUM BY QUINONES INDUCES RAPID CALCIUM EFFLUX. Jonathan J. Abramson, Edmond Buck, Guy Salama* (Intro. by J. Job Faber) Portland State University, Department of Physics, P.O. Box 751, Portland, OR 97207, and *Department of Physiology, University of Pittsburgh, Pittsburgh, PA 15261.

Quinones are known to play an important role in many electron transport system. Recently, Zorzato et al. (J. Biol. Chem. 260:7349) have shown that the quinone doxorubicin induces Ca^{2+} release from skeletal muscle SR and contraction in skinned muscle fibres. Here we show that the quinones, doxorubicin, menadione (vitamin K_3) and sodium anthroquinone-β sulfonate all induce rapid Ca^{2+} efflux from SR vesicles. Measurements of Ca^{2+} efflux are made using a Ca^{2+} sensitive electrode (WPI-Ca1 1) interfaced into an IBM-XT computer with a Tecmar analog to digital converter. Ca^{2+} efflux induced by these quinones is blocked by ruthenium red and high Mg^{2+}. Release is not observed with LSR vesicles or in the absence of adenine nucleotides. These findings indicate a relatively specific interaction with the Ca^{2+} release protein. Those quinones with the highest reduction potential are most effective in causing Ca^{2+} efflux, while in a reducing environment the quinones are ineffective in causing Ca^{2+} release. The addition of superoxide dismutase to remove oxygen free radicals does not inhibit Ca^{2+} release. The quinones tested appear to be causing Ca^{2+} release by oxidizing a group (perhaps a SH) associated with the Ca^{2+} release channel from sarcoplasmic reticulum. Supported by AHA, Alaska, Oregon and Western Penn. Affiliates of AHA and PSH RO1-NS18590. J.A. is an Established Investigator of AHA, G.S. is supported by RCDA-NS00909.

W-AM-C7 RAPID FILTRATION MEASUREMENTS OF Ca^{2+} RELEASE FROM CISTERNAL SARCOPLASMIC RETICULUM VESICLES. Carlota Sumbilla and Giuseppe Inesi. Department of Biological Chemistry, University of Maryland School of Medicine, 660 W. Redwood Street, Baltimore, MD 21201, USA.

A radioactive tracer and rapid filtration method was applied to the study of Ca^{2+} release from SR vesicles which were preloaded passively (equilibration with mM Ca^{2+}) or actively (in the presence of ATP). The method allows complete substitution of the loading mixture with release medium in constant flow, and time resolution between 10 milliseconds and 10.0 seconds. Net release can be clearly distinguished from isotope exchange. The latter is prominent in longitudinal SR vesicles. Net Ca^{2+} release is observed only from cisternal SR vesicles, is Ca^{2+} (micromolar) dependent, and is accelerated by inactive ATP analogues or ATP itself, even in the presence of Mg^{2+}. Net release has a strong pH dependence (between 6 and 7), and very little temperature dependence (consistent with a passive channel). In media of physiological significance (1 mM ATP, 1 mM magnesium, and free Ca^{2+} in the micromolar range), net Ca^{2+} release proceeds with a rate constant of approximately 100 sec^{-1}. This corresponds approximately to a 2×10^{-4} cm sec^{-1} Ca^{2+} permeability constant for cisternal SR. Although the mechanism of physiological gating is not known, the channel of cisternal vesicles is subject to regulation, since the rate of release is changed by 3-4 orders of magnitude following changes in Ca^{2+} and/or H^+ concentrations. (Supported by the USPHS and the Muscular Dystrophy Association).

W-AM-C8 IONIC REPLACEMENT-INDUCED CA^{2+} MOVEMENT ACROSS THE T-TUBULE MEMBRANE IN VITRO Alicia Ortega and Noriaki Ikemoto Dept. Muscle Res., Boston Biomed. Res. Inst., Boston, Mass. 02114, and Dept. Neurol. Harvard Med. Sch.

Recent studies (e.g. Curtis and Eisenberg, J. Gen. Physiol. 25, 383, 1985) suggest that the voltage-dependent influx of extracellular Ca^{2+} may be involved in e-c coupling. In an attempt to reproduce the equivalent processes in the purified T-tubules, we have investigated effects of creation and dissipation of the membrane potential on $^{45}Ca^{2+}$ uptake and release with the isolated T-tubule vesicles. The rate of ATP-dependent $^{45}Ca^{2+}$ uptake is much larger in the presence of an inside (=extracellular side)-positive potential (e.g. 75-135 mV) created by either a K^+ or Cl^- gradient than that at 0 potential. $^{45}Ca^{2+}$ uptake was carried out in the presence of an inside-positive potential (intravesicular solution- 190 mM choline Cl, 10 mM choline gluconate; extravesicular solution- 200 mM choline gluconate), and the membrane was depolarized by dilution with a solution containing 190 mM choline Cl, 10 mM choline gluconate. Upon membrane depolarization, 20-30% of the accumulated $^{45}Ca^{2+}$ was released within 20 s. Thirty uM D-600 produced partial inhibition (c. 60%) of the Ca^{2+} efflux induced by ionic replacement, suggesting that the efflux is mediated at least partly by the voltate-dependent Ca^{2+} channel. Details of the time course of Ca^{2+} efflux and the effects of various Ca^{2+} channel blockers on the kinetics of Ca^{2+} efflux are under investigation. (Supported by grants from NIH and MDA).

W-AM-C9 EFFECTS OF BETA-ADRENERGIC STIMULATION ON PHOSPHORYLATION OF MYOFILAMENTS, SARCOPLASMIC RETICULUM AND PHOSPHOLIPIDS IN PERFUSED GUINEA PIG HEARTS. G. Jakab*, S.T. Rapundalo*, R.J. Solaro+, and E.G. Kranias*. Departments of Pharmacology and Cell Biophysics* and Physiology and Biophysics+, University of Cincinnati, Cincinnati, OH

Beta-adrenergic stimulation alters functional dynamics of the heart by mechanisms most likely involving activation of cAMP-dependent protein kinases. In vitro studies indicate that cardiac myofibrils and SR may act as effectors of the beta-adrenergic stimulation. Studies are presented here in which guinea pig hearts were perfused with Krebs-Henseleit buffer containing ^{32}P-orthophosphate and freeze-clamped in a control condition or at the peak of the inotropic response to isoproterenol. Homogenates, myofibrils and microsomes enriched in sarcoplasmic reticulum (SR) were prepared from the same hearts. Stimulation of the hearts with isoproterenol was associated with increases in: a) cAMP levels, b) phosphorylation of troponin I and C-protein in myofibrils, c) phosphorylation of phospholamban in SR, and d) increased P_i-incorporation in phosphatidylinositol present in homogenates. Both phosphatidylinositol-4-phosphate and phosphatidylinositol-4,5, bis-phosphate were found to be phosphorylated in cardiac homogenates. These findings indicate that the effects of catecholamines on the mammalian heart may be due to an integrative response of several intracellular events. (Supported by NIH Grants HL26057, HL22231 and HL22619.)

W-AM-C10 ROLE OF THE 53 KILODALTON GLYCOPROTEIN OF THE SARCOPLASMIC RETICULUM. Howard Kutchai and Kevin P. Campbell, Department of Physiology, University of Virginia, Charlottesville, and Department of Physiology & Biophysics, University of Iowa, Iowa City.

We investigated the effects of an antiserum against the 53 KDa glycoprotein of the sarcoplasmic reticulum (SR) on Ca++ transport and ATP hydrolysis by SR of rabbit skeletal muscle. The antiserum had been produced in sheep immunized with purified 53 KDa glycoprotein by Campbell, Jorgensen, and MacLennan. The antiserum had been found to cross-react with the 160 KDa glycoprotein of SR, but not with the Ca-ATPase. Preincubation of SR with preimmune serum had no significant effect on either Ca++ uptake or ATP hydrolysis. Preincubation of SR with antiserum at 37 C resulted in decreased ATP-driven Ca++ uptake, but had no effect on Ca-stimulated ATP hydrolysis. The effect of antiserum on Ca++ uptake was time and concentration dependent. Half-maximal effect of antiserum required 30 min preincubation at 37 C. Two-fold dilution of antiserum resulted in significant reduction of its potency. Preincubation with antiserum did not increase the passive permeability of SR to Ca++ and did not cause proteolysis of the Ca-ATPase. Under our conditions, the estimated coupling ratio in control SR and in SR preincubated with preimmune serum was about 1.5 mole Ca++ transported/mole ATP hydrolyzed, while the coupling ratio in SR preincubated with antiserum for 60 min was 0.186. Our results are consistent with the interpretation that the 53 KDa glycoprotein may be involved in regulating the coupling of Ca++ transport to ATP hydrolysis by the Ca-ATPase of the SR membrane.

W-AM-C11 COMPLETE NUCLEOTIDE AND AMINO ACID SEQUENCE OF CANINE CARDIAC CALSEQUESTRIN. Bruce T. Scott[#,*], Larry R. Jones[#], John H. Collins[+] and Bernardo Nadal-Ginard[*]. [#]I.U. Sch. of Med., Indpls., In 46202, [+]Clarkson Univ., Potsdam, NY 13676 and [*]The Children's Hosp. Med. Cntr., Boston, MA 02115.

Calsequestrin, a Ca-binding protein found in junctional SR, is known to exist in cardiac and skeletal muscle as specific isoforms. We report here the determination of the complete nucleotide and derived amino acid sequence of the dog cardiac isoform. Calsequestrin was isolated from dog left ventricle by phenyl-Sepharose hydrophobic interaction chromatography. 44 N-terminal residues were directly sequenced by gas phase methods. A lambda gt11 cDNA expression library was constructed from dog left ventricle and screened with polyclonal antibodies generated to the purified cardiac protein. Antibody positive clones were rescreened with an oligonucleotide probe coding for the N-terminal sequence. A 2.6 kilobase cDNA clone was isolated and sequenced in both directions by the dideoxy method. The derived amino acid sequence contains 410 residues including a canonical 19 amino acid signal sequence. The protein does not exhibit sequence homology with other Ca-binding proteins and does not have the features characteristic of the EF hand. The amino acid sequence predicts long stretches of alpha helix and an unusual globular carboxy terminus containing 24 Asp residues out of 53. Several potential glycosylation sites are also contained within the primary structure. Experiments are currently in progress to determine with cardiac specific cDNA probes, if the cardiac form of calsequestrin is present in smooth muscle and slow skeletal muscle.

W-AM-D1 NUCLEOSIDE CONFORMATIONS OF VIRAL DNA IN FILAMENTOUS AND ISOMETRIC BACTERIOPHAGES INVESTIGATED BY RAMAN SPECTROSCOPY. Donna Sargent, Om P. Lamba, James M. Benevides and George J. Thomas, Jr., Department of Chemistry, Southeastern Massachusetts University, No. Dartmouth, MA 02747.

Results of DNA structure analysis from single crystal x-ray diffraction have been combined with laser Raman spectroscopy to identify characteristic conformation markers of the DNA Raman spectrum.[1] In favorable cases, the DNA Raman markers are diagnostic of both phosphodiester backbone geometry and nucleoside furanose pucker. The transferability of Raman data among samples of different morphology, especially crystals, fibers and solutions, permits use of the Raman method for identification of DNA conformations in non-crystallizable specimens, including viruses and other nucleoproteins. Applications to the following single-stranded DNA viruses will be discussed: filamentous phages of Class I (fd, If1, IKe) and Class II (Pf1, Xf, Pf3), and the isometric phage ØX174. Unusual DNA backbone geometries are found in all of these ssDNA phages. In addition, the nucleoside conformations prevalent in Class I and Class II filaments differ significantly from one another, while those of encapsidated ØX DNA are similar to the usual C2′endo/anti conformations of B form DNA despite evidence of a strained ØX DNA backbone. Variability of nucleoside conformation in ssDNA viruses contrasts with ssRNA viruses, for which the expected C3′endo nucleoside conformations are generally observed. Results on viruses will be discussed in relation to Raman data recently obtained from DNA crystals of the A, B and Z forms. (Supported by N.I.H. Grant AI11855.)

1. G. J. Thomas, Jr., J. M. Benevides and B. Prescott (1986) Biomolecular Stereodynamics 4, 227-253.

W-AM-D2 COMPARISON OF FD COAT PROTEIN IN ITS STRUCTURAL AND MEMBRANE BOUND FORMS, R.A. Schiksnis, M.J. Bogusky, L.A. Colnago, G.C. Leo, D.M. Schneider, P.L. Stewart, K.G. Valentine, and S.J. Opella

Filamentous bacteriophage coat protein exists in both structural and membrane bound forms during the viral life cycle. The structure and dynamics of the major coat protein of filamentous bacteriophage fd in both its intact and membrane bound forms have been characterized in order to help understand the phage assembly process and the various intermolecular interactions.

Solid state NMR studies on oriented phage particles whose coat protein has been biosynthetically ^{15}N or ^{13}C labeled yield the angular information necessary to describe the orientation of peptide planes, and, therefore, the conformation of the protein in its structural form. The NMR results indicate that the coat protein is helical. Protein backbone dynamics in the intact phage have been characterized by ^{15}N NMR; four amino terminal residues are mobile on the 10 kHz timescale. Side chain dynamics are studied by lineshape analysis of ^{2}H quadrupole powder patterns; most side chains studied undergo well defined motions on the 100 kHz timescale. The backbone dynamics of the coat protein in lipid bilayers has been characterized by ^{2}H and ^{15}N NMR; four amino and six carboxy terminal residues are mobile on the 10 kHz timescale. The structure of the coat protein in its membrane bound form is studied by applying solution NMR techniques to a detergent solubilized protein sample. Qualitative interpretation of NOESY spectra, in which amide proton resonances were assigned by $^{1}H/^{15}N$ shift correlation experiments, indicates that the coat protein spans the membrane in a helical conformation. The backbone dybamics of micelle bound coat protein have been characterized utilizing $^{15}N/^{1}H$ heteronuclear NOE experiments; four N-terminal and two C-terminal residues are mobile on the 10^{9} Hz timescale.

W-AM-D3 REFINEMENT OF THE STRUCTURE OF THE FILAMENTOUS BACTERIOPHAGE PF1
Raman Nambudripad & Lee Makowski
Dept. of Biochemistry & Molecular Biophysics, Columbia Univ. P&S, N.Y., NY 10032.

The structure of filamentous bacteriophage Pf1 is being studied by X-ray fiber diffraction. The virus consists of a large number of identical, 46 residue, protein subunits helically arranged around a circular single-stranded DNA molecule. Each protein is composed of two alpha-helical segments which form a double layer of alpha-helices about the DNA. From the 7Å resolution X-ray data, a preliminary rod model representing the alpha-helices has been proposed. A molecular model based on the data to a resolution of 3.5Å is now being built.

Recent developments in the analysis of fiber diffraction data and structure determination have enabled a molecular model for tobacco mosaic virus to be built to this resolution. Similar strategies are being adopted to arrive at a three-dimensional model for Pf1. A restrained least-squares method originally developed for crystal structures is being used for the refinement. High order Fourier synthesis is also being used to improve the molecular model. A model for Pf1 to 3.5Å resolution should resolve the ambiguity in chain tracing left by the 7Å model and allow elucidation of the protein-protein and protein-DNA interactions in the virion.

W-AM-D4 THREE DIMENSIONAL STRUCTURE OF FROZEN-HYDRATED CYTOCHROME c OXIDASE. E. L. Buhle, Jr.*, J.M. Murray**, and T.G. Frey***. Penn. Muscle Inst.*, Dept. of Anatomy**, U. of Penn Sch. of Med., Philadelphia, PA. and Dept. of Biology***, San Diego State Univ., San Diego, CA. (Intr. by A.M. Kelley)

Cytochrome c oxidase is the terminal enzyme complex of mitochondrial electron transport, mediating the transfer of electrons from reduced cytochrome c to oxygen. This transmembrane protein has been crystallized into small patches both within Triton extracted membranes (Type I) and by extraction with deoxycholate into another crystal form (Type II). Previous investigators have studied negatively stained crystals to a resolution of 2.5nm (1,2). In this study, these crystal forms have been imaged in the frozen-hydrated state. Type I crystals were imaged mostly in multilayer or 'onion-skinned' vesicles and had an average unit cell of a=9.4 and b=12.25nm. Type II crystals appeared to be one unit cell thick and had an average unit cell dimension similar to those found in negative stain. Both crystal forms contained local areas of highly ordered unit cells, but various degrees of long range disorder restricted these areas to rather small patches. The resolution in the best images is 1.5 nm, which is approximately the limit imposed by our cold stage. Supported by NIH HL07499 and NSF DMB8519677 (ELB), NSF DCB8415833, NIH RR01885 and RR01907 (JMM), and NIH GM38204 (TGF).

(1) Henderson et al., (1977) JMB 122:631-648.
(2) Fuller et al., (1979) JMB 134:305-327.

W-AM-D5 THE STRUCTURAL DOMAINS OF RIBOSOMAL PROTEIN L7/L12: PROTEOLYTIC DISSECTION AND CHARACTERIZATION OF FRAGMENTS. J. Christopher Corton and Kin-Ping Wong, Department of Biochemistry, University of Kansas Medical Center, Kansas City, KS 66103 and School of Natural Sciences, California State University, Fresno, Fresno, CA 93740.

Common fragments of ribosomal protein L7/L12 generated by several proteases were obtained which had molecular weights of 10,500, 8,500, and 7,000. Because the 10,500 and 8,500 fragments were dimeric in nature, the cleavages which produced these fragments were proposed to occur in the C-terminal end. Two fragments of a V8 protease digest, a dimer consisting of two 10,500 fragments and a 7,000 monomer were purified and their secondary structure and stability examined. All the data indicates the 7,000 fragment is composed of a very stable, highly helical N-terminal fragment whereas the 10,500 fragment is composed of the entire L7/L12 molecule except a region in the C-terminal end which has a much lower thermal stability. These results lend further support to the previously proposed molecular model of Luer and Wong (Biochem. 18, 2019-2027 [1979] and Biochem. 19, 178-183 [1980]) but are not consistent with the model proposed by Leijonmarck et al. (Nature 286, 824-826 [1981]). Further conformational studies of the protein in crystallization conditions used by Leijonmarck et al. show that the conformation is significantly different from its "native" conformation. (Supported in part by NIH grants GM 22962 and HL 33201.)

W-AM-D6 HIGH RESOLUTION ELECTRON MICROSCOPY OF NATIVE AND RECONSTITUTED AGGREGATES OF ALPHA CRYSTALLIN ISOFORMS

Jane F. Koretz, Biophysics and Biochemistry Group and Biol. Dept., RPI, Troy, NY, and Robert C. Augusteyn, Dept. of Biochemistry, University of Melbourne, Parkville, Victoria, Australia

Alpha-crystallin is a major protein component of the lenses of mammalian eyes, existing in situ as variably-sized aggregates of the 20 Kd subunits. If extracted at 4°C, the resultant particles (alpha-C) average about 800 Kd, while extraction at 37°C results in particles of about 240 Kd (alpha -M). The two isoforms of alpha crystallin - Alpha-A and Alpha-B - can each be reconstituted into aggregates of uniform size and molecular weight as determined by analytical untracentrifugation. As an initial step in the study of native and reconstituted alpha crystallin aggregates, the two "native" preparations and the two reconstituted aggregate types were examined in a Philips 420 TEM at 170,000 or 232,000X after negative staining with 2% aqueous uranyl acetate. Alpha-B and alpha-M crystallins are well-stained and exhibit some ultrastructural features, while alpha-A and alpha-C crystallins are poorly stained. Alpha-A particles are well formed spheres, with an average diameter of 84±13 A; aggregates of these particles with diameters up to 200 A can also be seen. Alpha-B particles, in contrast, show a single narrow distribution of spherical particles with average diameter of 91±12 A. Alpha-M crystallin also exhibits a narrow distribution of particle size with average diameter of 62±13 A, but the aggregate shape can be quite asymmetric. The alpha-C crystallin population appears to show a bimodal distribution; although the overall particle diameter average was 106±27 A, a second peak of 140 A average size was also discernible. The differences in size and stain sensitivity of the two "native" aggregates, despite the same A:B molar ratio, suggests a structural plasticity consistent with the much larger aggregates believed to exist in situ.

W-AM-D7 CHARACTERIZATION OF HYALURONATE SEGMENTS: EVIDENCE FOR SELF-ASSOCIATION IN 0.15M NaCl. R.E. Turner, P.Y. Lin, and M.K. Cowman, Department of Chemistry, Polytechnic University, Brooklyn, NY 11201.

Limited self-association of sodium hyaluronate (NaHA) in solution is postulated to result in formation of a molecular network. The existence of NaHA self-association has been investigated in the present study, using segments derived from the polymer by enzymatic digestion.

NaHA segments were purified by gel filtration chromatography. The molecular weight distributions and averages were determined by sensitivity-enhanced polyacrylamide gel electrophoresis (SE-PAGE). Samples A-G were found to have the following weight-average degrees of polymerization (number of repeating disaccharides): A, 90; B, 50; C, 38; D, 31; E, 23; F, 18; G, 13. The limiting viscosity number was determined for each sample in 0.15M NaCl. Results were correlated with the known weight average molecular weights, and the data were found to fit the relationship: $[\eta] = 6.54 \times 10^{-4} M^{1.16}$. Samples B-E were further analyzed by low angle laser light scattering. The apparent molecular weight in each case was equal to that determined by SE-PAGE, indicating no intermolecular association in the limit of low concentration. However, the second virial coefficient was found to be negative for the smaller segments (D and E), and positive for larger segments (B and C). The data are interpreted in terms of intermolecular association of short segments, but predominately intramolecular association (hairpin formation) for longer segments of NaHA. The overall extent of association, as judged by circular dichroism, increases with increasing molecular weight. NaHA segments should prove to be useful models for studies of the mechanism and thermodynamics of self-association. (Supported by NIH Grant EY 04804)

W-AM-D8 STRUCTURE AND ASSEMBLY OF FIBRIN CLOTS WITH DIFFERENT PROPERTIES. J.W. Weisel, Department of Anatomy, University of Pennsylvania School of Medicine, Philadelphia, PA 19104.

The structure and assembly mechanism of the formation of the fibrin clot have been investigated by electron microscopy. The physical characteristics of fibrin clots, which vary greatly with different conditions of formation, largely determine their stability and physiological and pathological interactions with other proteins and with blood. The structural basis of the wide variability of these properties has been studied by examination of clots formed by cleavage of either one or both pairs of fibrinopeptides from fibrinogen under a variety of different ionic conditions. Transmission electron microscopy of negatively contrasted clots revealed, unexpectedly, that most fibers, except those produced at both high ionic strength and pH, had about the same average diameter of 85 $\pm$ 13 nm. However, even in preparations of clots dispersed for microscopy, it was apparent that the degree of lateral aggregation of fibers with each other varied greatly. Thicker fiber bundles result at lower salt concentrations and pH and when both fibrinopeptides are cleaved. Scanning electron microscopy of intact clots has been used to measure the average diameters of the fiber bundles. In summary, in the assembly of the clot, two-stranded protofibrils, formed from the specific association of fibrin monomers after removal of either pair of fibrinopeptides, come together to make fibers of roughly constant diameter. These fibers then aggregate laterally to a variable extent, depending upon what fibrinopeptides have been cleaved and the ionic conditions.

W-AM-D9 ASSEMBLY OF TOBACCO MOSAIC VIRUS STUDIED BY TIME-RESOLVED SOLUTION X-RAY SCATTERING. Todd M. Schuster[1], Martin Potschka[1,2] Michel Koch[3] [1]Molecular and Cell Biology, University of Connecticut, Storrs, CT 06268, [2]Max Planck Institute for Biophysical Chemistry, Goettingen, Germany, [3]EMBL Outstation at DESY, Hamburg, Germany.

For several years it was thought that TMV coat protein (TMVP) assembles by two different paths at 0.1M ionic strength, to form either two layer cylindrical disks of 17 subunits per layer or helical rods of 16 1/3 subunits per turn (as in the native virus), depending on pH. Evidence has accumulated recently that the disk aggregate that crystallizes at high ionic strength does not exist in solution under virus assembly conditions and that the 20S protein which initiates assembly consists of about two turns of helically packed subunits. We have studied the kinetics of formation of 20S and larger helical rods of TMVP by temperature-jump time-resolved solution x-ray scattering to obtain radii of gyration of intermediate and equilibrium structures using a synchrotron x-ray source. Both the concentration dependence of the rate of formation of the 20S aggregate and the transient radius of gyration suggest that the minimum size nucleus for its formation consists of about 20 subunits and is a single layer structure, such as slightly more than one turn of a helix. Supported by NIH AI-11573.

W-AM-D10 EXOTHERMIC FIBRIL FORMATION OF TOBACCO MOSAIC VIRUS PROTEIN (TMVP) AGGREGATES.
K. Raghavendra and T. M. Schuster, Molecular & Cell Biology, Univ. of Connecticut, Storrs, CT 06268.

RNA-free TMV coat protein (TMVP) self-assembles to polymorphic aggregation states by an endothermic reaction. For the first time, we have obtained solution conditions which lead to exothermic TMVP polymerization. These consist of disk crystallization buffers, with 1.0M KCl instead of 0.3M ammonium sulphate originally used to obtain crystals of disk aggregates. In 1.0M KCl/Tris/HCl, pH 8.0 and 20°C, the state of aggregation is represented by the sedimentation boundary having an $s_{20,w}$ value of 36S. These aggregates (presumably stacks of 6-layers) readily dissociate when the solution conditions, such as pH, temperature and ionic strength are varied in contrast to the long term metastability exhibited by the ammonium sulphate stacks of disks (Raghavendra et al., Biochemistry, (1985),24, 3298; (1986), 25, October 7th issue). By cooling from 20°C to 5°C, the 36S aggregates dissociate to a mixture of 17S(70%) and 3S(30%); 17S may correspond to two layer disk aggregates. On standing at 5°C for >5 hrs, paracrystalline aggregates form resulting in strong turbidity, schleiren and phase separation of long macroscopic fibrils. Fibril formation has been followed by means of turbidity measurements, near-UV CD spectroscopy, optical and electron microscopy. These fibrils reversibly depolymerize to 36S aggregates slowly (> 2 days) when the temperature is raised to 20°C. The differences in the near-UV CD spectra of 17S, 36S and stacks of disks of TMVP have been interpreted in terms of differences in the packing polarity of the layers of subunits in these aggregates.
(Supported by NIH AI-11573).

W-AM-D11 THE PATHWAY OF SUBUNIT POLYMERIZATION DURING ICOSAHEDRAL CAPSID ASSEMBLY
Peter E. Prevelige Jr. and Jonathan King, Dept of Biology, MIT Cambridge, MA. 02139

The assembly pathway of subunits into icosahedral shells remains obscure. For Salmonella phage P22 efficient assembly of closed shells requires both coat and scaffolding protein subunits. These subunits have been purified in active form by dissociation of procapsids, the metastable double shell precursor of the capsid. The purified subunits do not self associate. Upon mixing of the coat and scaffolding proteins, and incubation at 24 °C, copolymerization to procapsid like double shells occurs. CD indicates the assembly process is accompanied by a conformational change.

To find structural intermediates in shell polymerization we have varied the scaffolding to coat ratio. The kinetics of this process were monitored by the change in turbidity. In the absence of scaffolding protein, coat protein remained monomeric. From scaffolding:coat ratios of 0.2:1 up to 1:1, the yield of procapsids increased linearly with scaffolding concentration. Above a 1:1 ratio the yield of procapsids was strongly inhibited. A new species was found, with a sedimentation rate less than that of the procapsid. This species appeared by EM to be incomplete shells. Addition of excess coat protein converted this species to closed shells. Thus, though scaffolding protein was required for initiation it inhibited elongation.

Consistent with this data is a pathway in which the subunits do not self associate in solution but rapidly and reversibly form a scaffolding/coat complex. Symmetry considerations suggest that three or five mixed oligomers then associate to form the initiating face or vertex. Growth proceeds at the edge of the complex by incorporation of uncomplexed coat and scaffolding monomers. High enough scaffolding to coat ratios would trap all the coat protein in scaffolding/coat complexes thereby preventing the elongation phase.

W-AM-D12 MECHANISM FOR PRODUCING TWO SYMMETRIES AT THE HEAD-TAIL JUNCTION OF BACTERIOPHAGES.
Philip Serwer, Department of Biochemistry, The University of Texas Health Science Center, San Antonio, Texas 78284-7760.

Some double-stranded DNA bacteriophages consist of a proteinaceous capsid that has an outer shell (head) that contains DNA; the head is attached to an external projection (tail). At the head-tail junction is a ring of subunits (connector) that has twelve-fold rotational symmetry. The head is made of subunits in either an icosahedral array or an array consisting of two icosahedral hemispheres separated by a cylinder of subunits. During infection of a host, the head with connector is assembled as a procapsid that subsequently packages DNA and joins a tail. In the mature bacteriophage, the twelve-fold symmetric connector is joined to the head at an axis of the head's five-fold rotational symmetry. The mechanism for producing two symmetries at the head-tail junction has been an unsolved problem (reviewed in [1]). The observation that the connector of bacteriophage T7 does not nucleate assembly of the head of T7's icosahedral procapsid (2) places a constraint on solutions of this problem. For icosahedral procapsids it is proposed here that: (a) Assembly of the head of the procapsid is nucleated by a six-membered ring of hexameric aggregates of the major head protein. (b) The connector is assembled in the center of this ring during assembly of the head. (c) One of the hexamers dissociates from the six-membered ring, creating a five-membered ring and forcing the connector to the inside of the head. This mechanism explains the grommet-like attachment of tails to mature heads, discussed in (1).

Refs.: (1) Bazinet, C., and King, J. (1985). Ann. Rev. Microbiol. 39,109.
(2) Serwer, P. and Watson, R.H. (1982). J. Virol. 42,595.

W-AM-E1 STRUCTURE OF THE REACTION CENTER FROM R. SPHAEROIDES AT 3.3 Å RESOLUTION.* J.P. Allen, G. Feher, U.C.S.D., La Jolla; T.O. Yeates, H. Komiya, and D.C. Rees, U.C.L.A., Los Angeles.

At last year's meeting we reported on the homology between the structures of RC from R. sphaeroides and R. viridis. We have now obtained the positions of the cofactors (see Fig.) and most of the amino acid residues at a resolution of 3.3 Å. The R factor between observed and calculated structure factors is 0.306. The data collection and analysis have been described (1,2). Completion of the positioning of the polypeptide chains and the collection of higher resolution data are in progress.

*Work supported by NIH and NSF

(1) J.P. Allen, G. Feher, T. O. Yeates, and D.C. Rees (1986) in Proc. of the VIIth Int. Cong. on Photosynthesis, in press. (2) J.P. Allen, G. Feher, T.O. Yeates, D.C. Rees, J. Deisenhofer, H. Michel, and R. Huber (1986) Proc. Natl. Acad. Sci., in press.

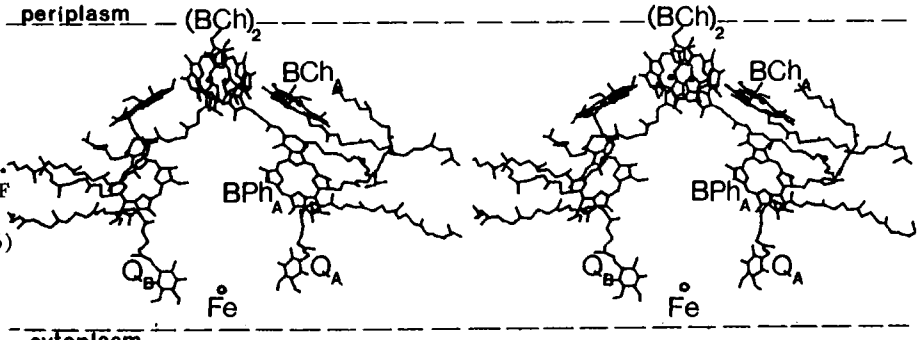

Stereoplot of the cofactors of the RC from R. sphaeroides at a resolution of 3.3 Å. The two-fold symmetry axis is aligned vertically in the plane of the paper. The electron transfer proceeds preferentially along the A-branch.

W-AM-E2 MAGNITUDE AND DIRECTION OF THE CHANGE IN DIPOLE MOMENT ASSOCIATED WITH EXCITATION OF THE PRIMARY ELECTRON DONOR IN R. SPHEROIDES REACTION CENTERS. David J. Lockhart and Steven G. Boxer, Department of Chemistry, Stanford University, Stanford California 94305

We have undertaken a quantitative analysis of the Stark effect on the absorption of R. spheroides RCs, inspired by the report of DeLeeuv et al. [Biophys.Soc.Abstr.37,111a(1982)]. We find that the change in dipole moment upon excitation of P870, $|\vec{\Delta\mu}|$, is f·(10±0.7)D, where f corrects for the local dielectric properties of the surrounding medium. Using the spherical cavity approximation and a dielectric constant of 2, f=0.83 and $|\vec{\Delta\mu}|$=8.3D. This value for $|\vec{\Delta\mu}|$ is substantially larger than expected for monomer BChl or that observed for the bands at 760 and 802nm. Data on the Q_x region will also be discussed. The angle, ζ, between $\vec{\Delta\mu}$ and the transition dipole moment at 870nm was measured by varying the angle, χ, between the E-vector of polarized light and the direction of the applied electric field (see data), giving ζ = 25°. The estimated angle between the Q_y transition moment of P870 and a vector between the Mg-atoms of each monomer in P870 (R. viridis structure assumed) is 20-30°. This result suggests that partial charge separation is occuring between the two halves of the special pair upon excitation. This may be the initial step in bacterial photosynthesis.

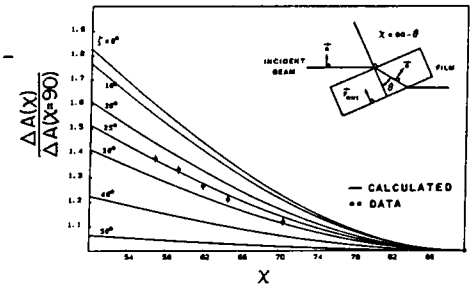

W-AM-E3 ENDOR OF THE REDUCED INTERMEDIATE ELECTRON ACCEPTOR IN RCs OF R. SPHAEROIDES.* G. Feher, R.A. Isaacson, M.Y. Okamura, U.C.S.D., La Jolla; W. Lubitz, Freie Universitaet, Berlin.

In previous EPR/ENDOR work it was shown that the intermediate acceptor radical anion I^- in RCs of R. sphaeroides involves a monomeric bacteriochlorophyll a or bacteriopheophytin, BPha. To improve our understanding of the electronic structure of I^- we have reinvestigated this species using an X-band spectrometer equipped with a loop gap ENDOR resonator, and obtained a considerably improved ENDOR spectrum (see Fig.). At least 14 hyperfine couplings (hfcs) were resolved; the two largest sets have been tentatively assigned to methyl protons on rings I and III. A preliminary analysis indicates that the spin density distribution of I^- is different from that of $BPha^-$ in ether. Two of the six line pairs detected in the Matrix region (see 10* and 12* in insert of Fig.) show a reduction in signal amplitude after incubation in D_2O. Consequently, we assign these hfcs to exchangeable protons on I^- or on nearby amino acid residues (e.g. Glu). Further experiments on specifically labelled RCs together with MO calculations are needed to fully interpret the data.

*Work supported by grants from NSF, DFG and NATO.

(1) G. Feher, R.A. Isaacson, M.Y. Okamura, Biophys. J. (1977) 17, 149a. (2) W. Lubitz, F. Lendzian, K. Moebius, Chem. Phys. Lett. (1981) 84, 33.

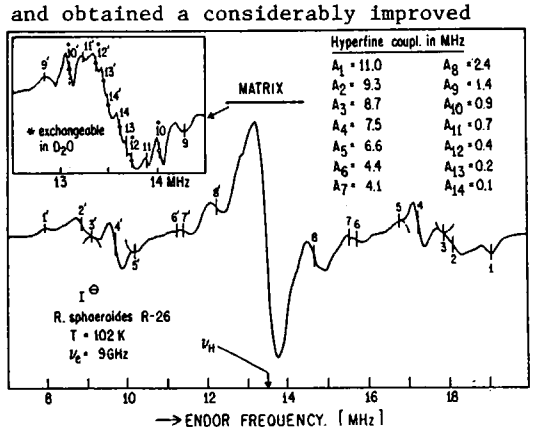

W-AM-E4 ENDOR CHARACTERIZATION OF BIOLOGICAL QUINONES. Christopher J. Bender[a], Ivan D. Rodriquez[a], Wolfgang Lockau[b], Gerald T. Babcock[a], [a]Department of Chemistry, Michigan State University, East Lansing, MI 48824-1322. [b]Universität Regensburg, 8400 Regensburg, FR Germany.

Recent data suggest that the A_1^- signal in PSI is due to a menaquinone. Powder ENDOR spectra of both PSI particles and substituted napthoquinones have been recorded in frozen solutions. Comparison of the spectra obtained for the biological material with those of the model quinones permits the assignment of hyperfine couplings and enables the identification of the A_1^- radical. Isotropic and anisotropic hyperfine interactions of methyl and hydrogen bond protons have been measured for menadione and menaquinone neutral and anion radicals. For the menaquinone anion radical the anisotropic hyperfine interactions are found to be $A_\perp$ = 2.94MHz for a hydrogen-bonded proton; $A_\parallel$ is expected at 5.9MHz for this dipolar coupled proton but it is obscured by $A_\perp$ of the methyl proton. From these data the istropic hyperfine interaction, 1/3 ($A_\parallel$+2$A_\perp$), is 7.77MHz for the methyl proton in agreement with the experimental value of 7.7 MHz we obtained from liquid solution ENDOR. In the ENDOR spectrum of the A_1^- radical we assign $A_\perp$ = 4.76MHz and $A_\parallel$ = 7.46MHz to the hyperfine interaction of the methyl protons. The $A_\perp$ component of a hydrogen-bonded proton is apparent at 2.07MHz and although $A_\parallel$ for this dipolar-coupled proton is expected at 4.2MHz, the precise position of this feature is obscured by $A_\perp$ of the methyl. Finally, a derivative shaped feature is observed with the splitting of 9.31MHz, comparison with model compounds indicates a similarity to hydroxyl proton hyperfine. Our findings are consistent with the identification of the A_1^- species of PSI with a menaquinone radical. Supported by (NIH GM-37300)

W-AM-E5 ELECTRON TRANSFER IN RHODOPSEUDOMONAS SPHAEROIDES REACTION CENTER PROTEIN WITH LOW POTENTIAL QUINONES AS Q_A. M.R.Gunner, D.E.Robertson, R.LoBrutto, A.McLaughlin, and P.L.Dutton. Dept of Biochem and Biophys, U of Pa. Phila, Pa. 19104

The quantum yield for $(BChl)_2^+Q_A^-$ formation (phi) was was determined by light saturation in RCs where the native Q_A, UQ_{10}, was replaced by other quinones. For quinones of in situ $E_{1/2}$ >0.15 eV lower than UQ_{10}, phi decreases with $E_{1/2}$, implying that electron transfer from BPh^- to Q_A slows, thereby increasing $(BChl)_2^+BPh^-$ lifetime so that competing electron transfer from BPh^- to $(BChl)_2^+$ becomes significant. Phi is temperature independent (5-300K). A rate decrease with decreasing $-\Delta G^0$, also without temperature sensitivity, is also found for electron transfer from Q_A^- to $(BChl)_2^+$ (M.R.Gunner, et.al. J.Phys.Chem. (1986) 90, 3783-3795)

A light-generated, spin-polarized EPR signal (SP) is found when Q_A $E_{1/2}$ is >0.10 eV lower than UQ_{10}. SP shows emission and a more intense high field absorption centered near g=2.003 which decays at 4000/s (6K) or >30,000/s (113K). This rate (6K) is equal to the T_1-dependent appearance of the $(BChl)_2^+$ signal (g=2.0026) in RC where SP is not visible and, in RC with SP, at fields near g=2.003 where the amplitude of SP is ~0 and the $(BChl)_2^+$ signal is maximal. The largest ratio of signal amplitudes of SP absorption to $(BChl)_2^+$ (2-Et-AQ as Q_A) is ~ 4 (6K) or ~30 (113K). SP amplitude increases as phi decreases but no SP is seen when no $(BChl)_2^+Q_A^-$ is formed, so increasing lifetime of $(BChl)_2^+BPh^-$ prior to $(BChl)_2^+Q_A^-$ formation may be required for SP generation. Supported by NSF PCM 09202.

W-AM-E6 CHLOROPHYLL MODEL COMPOUNDS: RESONANCE RAMAN SPECTRA AND NORMAL MODE DESCRIPTIONS FOR NI(II) DIHYDROPORPHYRINS. Nancy J. Boldt, Robert J. Donohoe, Robert R. Birge and David F. Bocian, Department of Chemistry, Carnegie Mellon University, Pittsburgh, PA 15213

Resonance Raman spectra are reported for a series of Ni(II) dihydroporphyrins with excitation in the B, Q_x and Q_y absorption regions. The molecules include trans-octaethylchlorin and several pyropheophorbides. These molecules represent a series in which the structural complexities of chlorophyll a (reduced pyrrole ring, isocyclic ring, 9-keto group and 2-vinyl group) are systematically added to the basic tetrapyrrole structure. All of the observed in-plane chlorin skeletal modes and vibrations of the isocyclic ring and vinyl group are assigned. Assignments are then proposed for chlorophyll a based on analogy to those of the Ni(II) complexes. In addition to the spectral assignments, normal coordinate calculations are performed on the various Ni(II) dihydroporphyrins. These calculations indicate that the forms of the normal coordinates of the metallochlorins bear little resemblance to those of the parent metalloporphyrins. In the low-symmetry environment which characterizes the reduced-pyrrole pigments, a number of the vibrations are localized in hemispheres or quadrants of the macrocycle rather than being delocalized over the entire ring. This vibrational localization is due to geometrical changes in the π-bonded system which occur as a result of reduction of one of the pyrrole rings and addition of the isocyclic ring. The localization may have a significant effect on the magnitude of intermolecular vibronic coupling which can occur between chlorophyll molecules in the special pair.

W-AM-E7 EFFECTS OF PROTEIN SOLVATION ON THE PROPERTIES OF (BACTERIO)CHLOROPHYLLS. THEORETICAL STUDIES. L.K. Hanson and J. Fajer. Department of Applied Science, Brookhaven National Laboratory, Upton, New York 11973.

Recent x-ray data for bacterial reaction centers have revealed the spatial organization and protein environment of the chromophores involved in the primary photosynthetic charge separation.[1] The bacterio-chlorophylls and-pheophytins are arranged in two arms, related by an approximate twofold axis, only one of which is active. The protein residues surrounding the pigments in the two arms differ resulting in different "solvation" and hydrogen bonding in the active and inactive pathways. Extended Hückel and INDO calculations are used to consider the effects of axial ligation (imidazole and imidazolate), hydrogen bonding, and substituent orientation on the optical and redox properties of the bacteriochlorophylls as well as on the unpaired spin densities of the radicals generated by the primary charge separation. Similar environments are assumed for green plant reaction centers and calculated for the chlorophylls of photosystems I and II.

Although the "solvation" effects are shown not to be large, in agreement with experimental data, small asymmetries in the protein environments of the bacterial primary donors may be sufficient to determine the direction of electron flow in the nascent charge separation and thus discriminate between the two possible electron pathways discerned the x-ray data of the reaction centers.

This work supported by the Chemical Sciences Division of the U.S. Department of Energy.

(1). Deisenhofer et al. Nature 318, 618 (1985); Chang et al. FEBS Letters 205, 82 (1986).

W-AM-E8 ESR RELAXATION STUDIES ON SIGNALS FROM PLANT PS-II. R.J. Pace, D. Stehlik* and R. Bramley, Research School of Chemistry, Australian National University, Canberra A.C.T. Australia 2601. *On leave from Free University, Berlin.

The relaxation properties of the multiline S_2 state signal induced in spinach PS-II particles by cryogenic illumination has been studied. Two classes of behaviour have been found in 200 K green light (500-550nm) illuminated samples, depending on treatment prior to freezing, which appear to correspond to the 'active' and 'resting' forms identified by Brudvig et al (Biochemistry 24, 3085). The resting state (long dark adapted) signal intensity falls with decreasing temperature near 4 K, but careful power saturation studies show that this is not due to a loss of spin population, but a purely saturation effect. The signal amplitude at limitingly small power shows Curie behaviour down to 4 K. 'Active' state signals, formed from samples pre-illuminated at 20°C with green light, also show Curie behaviour but with a greatly enhanced relaxation rate at ~4 K and with the downfield components of the multiline spectrum saturating less readily than the upfield components. This difference is consistent with a dipolar interaction between the multiline centre and a low field species, and a previously unreported broad feature of variable g value between 3 and 4 is present in these samples. Further, signal IIs shows significantly enhanced relaxation in the presence of this feature, suggesting again dipolar interaction between the centres but over a substantially larger distance than for the multiline case. The g 3-4 signal is variable in shape but sometimes resembles the 4.1 signal. Like the latter it anneals away at 200 K and its formation is inhibited by alcohol. Possible origins of this new signal will be discussed.

W-AM-E9 THE RATE OF FORMATION OF $P700^+ - A_0^-$ IN PHOTOSYSTEM I PARTICLES FROM SPINACH AS MEASURED BY PICOSECOND TRANSIENT ABSORPTION SPECTROSCOPY. M.R. Wasielewski, Chem. Div., Argonne National Laboratory, Argonne, IL. 60439 and J. Fenton and Govindjee, Depts. of Plant Biology, Physiology, and Biophysics, University of Illinois, Urbana, IL. 61801

PS I particles containing 30-40 Chl molecules per P700 were subjected to 1.5 ps laser flashes at 610 nm resulting in excitation of the antenna Chl molecules followed by energy transfer to P700 and subsequent oxidation of P700. Absorbance changes were monitored as a function of time with 1.5 ps time resolution. P700 bleaching occurred within the time resolution of the experiment. This is attributed to the formation of ^{1}*P700. This observation was confirmed by monitoring the rise of a broad absorption band near 810 nm due to Chl excited singlet state formation. The appearance of the bleach at 700 nm was followed by strong bleaching at 690 nm. The time constant for the appearance of the 690 nm bleach is 13.7 ± 0.8 ps. In the near-infrared region of the spectrum the 810 nm band which formed upon excitation of the PS I particles diminished to about 0.6 of its original intensity with the same 13.7 ps time constant as the formation of the 690 nm band. The spectral changes are interpreted as due to the formation of $P700^+ - A_0^-$.

This work was supported by the Division of Chemical Sciences, Office of Basic Energy Sciences of the U.S. Department of Energy under contract W-31-109-Eng-38.

W-AM-E10 THE EFFECT OF INTERNAL BUFFERS ON PHOTOPHOSPHORYLATION AND POSTILLUMINATION PHOSPHORYLATION IN CHLOROPLASTS AND SUBCHLOROPLAST PARTICLES. R.D. Horner and E.N. Moudrianakis, Biology Dept., The Johns Hopkins Univ., Baltimore, MD 21218. In chloroplasts treated with valinomycin and K^+, the initial development of photophosphorylation and postillumination phosphorylation was measured in the presence or absence of permeant amine buffers through the use of rapid-mix, acid-quench techniques. In the absence of permeant buffers, both processes appeared to initiate after the same illumination interval. In the presence of these buffers, the initiation of postillumination phosphorylation was delayed, but the intiation of photophosphorylation was not. These results indicate that postillumination phosphorylation is driven by protons from the inner aqueous space of the chloroplast thylakoid which are affected by permeating buffers. However, photophosphorylation appears to be supported by protons which are sequestered from the inner aqueous space. Subchloroplast particles made by sonication in the presence of MES buffer have MES within the vesicles as shown by direct titration and stimulation of light-induced proton uptake and postillumination phosphorylation. Preliminary results show that the internal MES within these vesicles has the same effects as permeant amine buffers do in whole thylakoids, indicating that these effects are not due to uncoupling artifacts. Because neither localized nor delocalized models of proton coupling can account for these observations, we propose that a gating mechanism exists which partitions intramembrane protons initially to the ATP synthetase complex and to the lumen. (Supported by a grant from NSF)

W-AM-F1 ANALYSIS OF IRREVERSIBLE TRANSITIONS USING DIFFERENTIAL SCANNING CALORIMETRY.
Ernesto Freire, Department of Biology, The Johns Hopkins University, Baltimore, MD 21218.

The thermal stability of several multidomain proteins, multisubunit proteins, and membrane proteins is currently being investigated by high sensitivity differential scanning calorimetry in various laboratories. Contrary to the case of small globular proteins, the thermal unfolding of these large proteins or protein complexes is, under most conditions, characterized by complex profiles showing little or none reversibility. In many cases this irreversible behavior is characterized by the presence of exothermic heat effects that partially overlap or immediately follow the endothermic peak(s) associated with the denaturation process. This irreversible behavior is generally associated with processes of the type $F \rightleftharpoons U \longrightarrow P$ in which the unfolded state of the protein (U) irreversible transforms into a post-equilbrium state P. The purpose of this communication is to examine the properties of these irreversible denaturation processes and to develop a series of experimental tests directed to determine the type of information that can and cannot be obtained from calorimetric studies of these systems. (Supported by NIH grant GM-37911).

W-AM-F2 THE THERMAL STABILITY OF GLOBULAR PROTEINS. Ken A. Dill and Karen Hutchinson, Pharmaceutical Chemistry, University of California, San Francisco, CA 94143.

For many years, the thermal denaturation of proteins has posed a paradox: since the hydrophobic effect strengthens with temperature, proteins should fold more tightly, rather than denature, upon heating. We consider here theory for the balance of forces which stabilize globular proteins. The hydrophobic effect drives the molecule toward the condensed state; the chain conformational entropy drives the molecule toward the unfolded state. Using experimental values for the temperature dependence of the oil/water transfer of amino acids, taken from Tanford and Nozaki, and Gill and Wadso, and otherwise no adjustable parameters, the theory well predicts the experimental values of the enthalpy, entropy, and free energy of folding of small globular proteins measured by Privalov and Khechinashvili. The theory predicts two first order phase transitions: one at the normal denaturation temperature, and a "cold denaturation" at lower temperatures. The paradox above is resolved by accounting for the chain conformational entropy.

W-AM-F3 DENATURATION THERMODYNAMICS AS A TOOL IN STUDYING ENZYME MEDIATED REACTIONS--Marcelo M. Santoro and D. W. Bolen, Dept. of Chem. & Biochem., Southern Illinois Univ., Carbondale, IL 62901.

The free energy change for protein unfolding reflects the magnitude of the difference between noncovalent interactions among various parts of the protein and the interaction of these parts with solvent. In principle, unfolding free energy changes may be used to quantitate differences between closely related proteins such as would occur between a native enzyme and a covalently modified form of the enzyme created during the course of catalysis. Use of such free energy differences complements the free energy diagram of the enzyme catalyzed reaction in such a way as to provide the possibility of extracting unique thermodynamic quantities concerned with the catalytic process. Such treatment requires accurate assessment of the unfolding free energy change along with the accompanying error. It also requires finding conditions (such as low pH) which stabilize the covalent enzyme-substrate species, thus making it possible to evaluate the unfolding free energy change. An assessment of the feasibility of this approach is presented for a prototype covalent enzyme-substrate intermediate, phenylmethanesulfonyl-chymotrypsin. The procedure for evaluating the unfolding free energy change in the pH range where the enzyme is catalytically active will also be presented and discussed.

W-AM-F4 EFFECT OF CHARGED SIDE CHAINS ON THE DNA BINDING OF INTERCALATORS. Luis A. Marky, Wan Y. Chou, Denise Zaunczkowski, and Kenneth J. Breslauer. Department of Chemistry, Rutgers University, New Brunswick, NJ 08903.

Ethidium and propidium cations are important drugs whose biological effects are of general interest. Both drugs contain an aromatic phenanthridinium ring system, but differ by the nature of the attached substituent group. Propidium contains a large, charged side chain in contrast with the neutral ethyl group of ethidium. Both drugs bind to DNA and RNA by intercalation of the aromatic rings. To investigate the influence of the charged side chain of propidium on the binding affinity and specificity, we have used a combination of absorption spectrometry and calorimetry to characterize thermodynamically the binding of both drugs to poly dAT•poly dAT ("B" conformation) and to poly rA•poly rU ("A" conformation). In 10mM phosphate buffer, pH = 7.0 we obtained the following thermodynamic binding profiles at 25°C.

duplex	drug	ΔG (kcal/mol)	ΔH (kcal/mol)	ΔS (cal/mol-°K)	$\partial \log K / \partial \log Na^+$
poly dAT•poly dAT	ethidium	-9.1	-10.0	-3	-0.83
	propidium	-10.5	-5.5	17	-1.85
poly rA•poly rU	ethidium	-8.7	-9.0	-1	-0.85
	propidium	-11.3	-8.1	11	-1.83

Based on the above results, we can draw the following conclusions:

1) Propidium binds more strongly than ethidium to both the "B" and the "A" duplex. This differential affinity is more pronounced with the "A" duplex. 2) For both duplexes, the enhanced binding of propidium is due to a more favorable entropy. 3) Propidium exhibits a less favorable binding enthalpy when it complexes with the "B" duplex compared to when it complexes with the "A" duplex. 4) The "B" duplex enthalpically discriminates between the two drugs more than the "A" duplex. 5) Duplex conformation does not alter the electrostatic contribution to the binding of either drug. We are now studying the binding of the drugs to poly dA•poly dT and poly rAU•poly rAU duplexes to evaluate if the effects we have observed are due to differences in homo versus alternating sequences. This work is supported by NIH Grant GM34469.

W-AM-F5 ROLE OF MACROMOLECULAR ASSEMBLY IN THE REGULATION OF PHOSPHOFRUCTOKINASE. James C. Lee, Guang-Zuan Cai, and Michael A. Luther, Department of Biochemistry, St. Louis University School of Medicine, St. Louis, MO, 63104.

The steady-state kinetic behavior of rabbit muscle phosphofructokinase (PFK) varies with protein concentration. At low protein concentration, the relation between activity and substrate concentration is sigmoidal, whereas at higher PFK concentration, it is hyperbolic. Hence, the self-assembly of PFK subunits is related to the basic kinetic behavior of the enzyme. Sedimentation velocity studies show that the association and dissociation of PFK subunit can be characterized as rapid, and the oligomeric forms are in dynamic equilibrium. The overall mode of association is $M_1 \rightleftarrows M_2 \rightleftarrows M_4 \rightleftarrows M_8 \rightleftarrows M_{16}$. Enzymic activating conditions favor the formation of the aggregated species, whereas inhibitory conditions reverse the process. Substrates will not only enhance subunit assembly, but also induce a global structural change in the tetrameric form of PFK. Besides being regulated by small ligands and subunit assembly, PFK activity can be affected by other macromolecules, such as F-actin. The latter interaction is affected by phosphorylation of PFK. In summary, the enzymic activity of PFK is regulated by macromolecular assembly, which in turn is affected by metabolites.

W-AM-F6 **NEW DETERMINATION OF OXYGEN BINDING CONSTANTS FOR HUMAN HEMOGLOBIN TETRAMERS**

Stanley J. Gill, Gary Bishop, Enrico Di Cera, Michael Doyle and Charles H. Robert
Department of Chemistry and Biochemistry, University of Colorado, Boulder, CO 80309

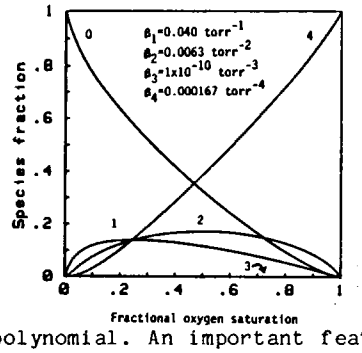

Employment of differential measurements of oxygen binding to human hemoglobin at high concentrations (4-12 mM heme) has led to the unexpected conclusion that the singly and doubly ligated intermediate species make a much greater contribution to the oxygen binding curve than the triply ligated species, which is practically unmeasurable. High precision measurements were made using a thin-layer apparatus of oxygen binding to hemoglobin HbA_o under a variety of solution conditions. Each step of an experiment consists of measuring the change of optical density resulting from a precise change in the oxygen partial pressure. The sample is thus taken from one equilibrium state to another. With the use of high concentrations the effects of tetramer dissociation can be neglected and analysis of the binding reactions can be cast in terms of the simple Adair binding polynomial. An important feature in the analysis was the expression of the binding equilibria as overall reactions ($Hb + i\ O_2 \rightarrow Hb(O_2)_i$), which results in lower correlation and higher resolution in the fitting process. Experiments conducted under a variety of conditions indicate a strongly asymmetric distribution of ligation intermediates (shown in figure for pH 7.5, 0.1 M phosphate), where the triply ligated species appears to be negligible. Supported by NIH grant HL 22325.

W-AM-F7 STRATEGIES FOR USING MUTANTS TO STUDY FUNCTIONAL ENERGETICS OF PROTEINS.
Gary K. Ackers and Francine R. Smith, Dept. of Biology, Johns Hopkins Univ., Balto., MD 21218.

A general approach to protein structure-function issues called "mapping by structure-function perturbation" will be discussed. In this strategy a series of mutant or chemically-modified proteins are characterized functionally as to their deviation from normal behavior (i.e., their functional perturbation). The magnitudes of functional perturbations are analyzed in relation to the structural locations of the modification sites. Thus a mapping is obtained for the regions of the molecule that are sensitive to local structural alterations in terms of a given function. When function can be related to thermodynamic parameters (e.g., Gibbs energy of molecular interaction) the approach can be extended to combinations of various single-site modifications to determine the pathways of internal coupling between sites and sub-regions of a molecular structure as expressed in terms of function. The method has special value for multi-subunit, multi-functional proteins that exhibit cooperativity such as allosteric proteins. By mapping the functional perturbations directly against structural locations one can bypass the difficulties of attempting to translate the atomic-level interactions into complex functional behavior.

The strategy outlined above does not replace the more traditional approach of analyzing the local stereochemistry of the structural modification, but provides a complementary approach. Recent applications of mapping by structure-function perturbation will be discussed. Supported by grants from the NIH and NSF.

W-AM-G1 STABILIZATION OF THE $Mg \cdot E_1$ CONFORMATION OF Na^+,K^+-ATPase BY MONOCLONAL ANTIBODY BINDING. Mark L. Friedman and William J. Ball, Jr., Department of Pharmacology and Cell Biophysics, University of Cincinnati College of Medicine, Cincinnati, OH 45267.

Monoclonal antibody 9-A5, raised against rat kidney Na^+,K^+-ATPase (Schenk, and Leffert, PNAS USA 80: 5281, 1983) has been found to inhibit the lamb kidney enzyme ATPase and pNPPase activities. The mechanism of inhibition was investigated by monitoring antibody effects on ligand-induced fluorescence changes undergone by the FITC-labeled enzyme. We have found that 9-A5 binding causes a 25% increase in FITC fluorescence and an enhancement of the Na^+-induced increase accompanying the $E_2 \rightarrow Na^+ \cdot E_1$ transition. 9-A5 also diminishes the fluorescence change of the $E_1 \rightarrow K^+ \cdot E_2$ interconversion, causes an increase (37%) in fluorescence when added to $K^+ \cdot E_2$, and reduces enzyme affinity for K^+ about 10-fold. These effects are similar to those of Na^+ and suggest a 9-A5-induced stabilization of the E_1 conformation. In the presence of Mg^{2+}, 9-A5 prevents the $E_1 \rightarrow E_2$ conversion induced by K^+, P_i or ouabain. However FITC fluorescence was quenched ~58% when Mg^{2+},P_i and ouabain were combined. Together the three ligands overcame the 9-A5 caused inhibition by apparently promoting the dissociation of bound antibody. These results suggest that 9-A5 binds to a region of the α subunit at or near the phosphorylation site which is involved in the $E_1 \rightleftarrows E_2$ transitions. Inhibition of enzyme activity most likely occurs by inhibition of E_2P formation. In agreement with our conclusions, Farley et al. (Am. J. Physiol. 250: 896, 1986) have shown that 9-A5 binds the chymotryptic fragment C(35) containing the phosphorylation site and a portion of the putative ouabain binding site (Supported by NIH Grants T32-HL-07382 and RO1-HL-32214. WJB is an Established Investigator of the American Heart Association).

W-AM-G2 LOCATING ANTIGENIC DETERMINANTS OF THE α-SUBUNIT OF Na^+,K^+-ATPase. William J. Ball, Jr. and Charles D. Loftice, Department of Pharmacology and Cell Biophysics, University of Cincinnati College of Medicine, Cincinnati, OH 45267.

Determination of the tertiary structure of Na^+,K^+-ATPase is essential for understanding its mechanism of action. The complete amino acid sequence of the α subunit of lamb kidney Na^+,K^+-ATPase has recently been obtained and used to make predictions of its secondary and tertiary structure (Shull et al., Nature 316: 691, 1985). In order to immunologically identify the predicted exposed regions of α, rabbit antisera were raised against a series of synthetic peptides corresponding to different sequence regions of α. Five of six peptides tested (11-15 amino acid residues in length) were immunogenic and the antisera to four peptides recognized the intact, transblotted α. Immunization of rabbits with peptides conjugated to keyhole limpet haemocyanin (KLH) produced peptide-directed antibodies for six of eight peptides, with the majority of the antisera binding to transblotted α. In addition, antisera to three of the conjugated peptides recognized the native enzyme demonstrating that these sequence regions are exposed in the holoenzyme. These synthetic peptides were then tested as antigens for a collection of antisera and monoclonal antibodies raised to native holoenzyme. Sequence regions 16-30, near the NH_2-terminal end, and 496-506, the putative ATP binding site, were recognized by enzyme-directed antibodies and therefore identified as both immunogenic and antigenic determinant sites of α. The studies demonstrate that short synthetic peptides can be used to map antigenic sites of this membrane bound enzyme. (This work was supported by NIH grants RO1 HL32214 and PO1 HL22619. WJB is an Established Investigator of the American Heart Association.)

W-AM-G3 MECHANISM OF INACTIVATION OF RENAL Na,K-ATPase BY H_2DIDS. C.H. PEDEMONTE & J.H. KAPLAN. Dept. of Physiology, Univ. of Pennsylvania, Phila., PA 19104.

We previously reported that treatment of renal Na,K-ATPase with 4,4'-diisothiocyano-1,2-diphenylethane-2,2'disulfonic acid (H_2DIDS) results in inhibition of Na,K-ATPase and K-phosphatase activities (Biophys. J. 49:35a, 1986). The enzyme is reversibly or irreversibly inhibited depending on the presence or absence respectively of physiological ligands. Inactivation kinetics are first order with respect to time and [H_2DIDS] suggesting that covalent reaction at one site in the enzyme was sufficient to remove activity. The extent of inhibition of modified enzyme correlated with the decrease in high affinity ATP binding, phosphorylation by P_i was unaffected. Estimates of covalent binding of $^3H_2$DIDS showed that reaction of one H_2DIDS molecule per phosphorylation site inactivated the enzyme. SDS PAGE analysis of the modified protein showed label was only on the α subunit. Complete inactivation was accompanied by the incorporation of 6.1 and 3.6 nmol of H_2DIDS per mg of protein at pH 7.2 and 9.1, respectively. Reversible inhibition is reduced as the pH is raised from 6.5 to 8.5. The H_2DIDS binding domain has an array of titrable groups, the initial interaction between charged groups whose pK>6.5 and the sulfonic acids results in reversible inhibition. Subsequently covalent reaction between the NCS of reversibly bound H_2DIDS and a conformationally sensitive NH_2 group on the enzyme results in irreversible inhibition. Supported by NIH HL 30315 and RCDA HL 01092.

W-AM-G4 A TEST OF THE OCCLUSION HYPOTHESIS ON THE SODIUM PUMP IN HUMAN RED CELLS. L.J. KENNEY & J.H. KAPLAN. Dept. of Physiology, Univ. of PA. Phila, PA 19104.

In 1972, Post observed that the rate limitation of Na,K-ATPase at low [ATP] was relieved by elevated [ATP] (Post et al, J.Biol.Chem. 247:6530). They concluded that a stable occluded cation-enzyme form was produced following dephosphorylation by K and that ATP, acting with a low affinity, accelerated release. This occluded form has become an important intermediate in current models of the hydrolytic and transport pathways of the sodium pump. In the K:K exchange transport mode in human red cells, the P_i and nucleotide requirements are believed to reflect the acceleration and release of K from an occluded state $E_2(K)$ to the external medium (P_i) or to the cytosol (ATP & ADP). We have shown that Li (not occluded by the Na pump) will substitute for K at the intracellular site, supporting ouabain-sensitive ^{86}Rb uptake (Biophys.J.49:37a, 1986). We were interested in testing some predictions of the occlusion hypothesis on sodium pump-mediated transport. Resealed red cell ghosts were prepared by gel filtration containing 50mM Li or Rb and the effect of intracellular ADP or P_i on the ^{86}Rb uptake was determined. When Rb was the internal cation, ADP and P_i stimulated ^{86}Rb influx. However, in ghosts containing Li, ADP stimulated the influx whilst P_i was without effect. When ^{86}Rb efflux was measured into Li, P_i stimulated the efflux and ADP was without effect. These data confirm that, when deocclusion to the cytosol is rate limiting, ADP accelerates release and when deocclusion to the extracellular medium is limiting, P_i accelerates release. Support: NIH HL30315 & RCDA HL01092.

W-AM-G5 EFFECT OF PH ON CATALYSIS OF MEDIUM OXYGEN-18 EXCHANGE BY THE GASTRIC H,K-ATPASE. Larry D. Faller, CURE/UCLA, Veterans Administration Wadsworth Hospital Center, Los Angeles, CA 90073.

The K^+-stimulated, H^+-translocating ATPase isolated from gastric mucosae catalyzes oxygen-18 exchange between inorganic phosphate and water by reversal of the terminal steps in ATP hydrolysis (Faller & Elgavish, Biochemistry 23, 6584, 1984). Therefore, the effect of pH on medium exchange can be used to assess the role of protons in the catalytic/transport mechanism. The temporal distribution of labeled species, as oxygen-18 exchanges out of 96% enriched inorganic phosphate, has been measured by 31-P NMR (Cohn & Hu, PNAS 75, 200, 1978) and compared to ATPase activity in the pH range 7.4 to 6.0. Both activities decrease monotonically with pH, but the isotope exchange rate decreases only one-third as fast as the hydrolysis rate. The rate of disappearance of fully-labeled phosphate decreases twice as fast with pH as the rate of loss of average isotope enrichment. Therefore, the average number of oxygen atoms exchanged per turnover increases as the pH is lowered. This means that the rate of enzyme phosphorylation increases relative to the rate of inorganic phosphate loss from the enzyme and suggests that the reactive form of the enzyme is protonated. It strengthens the interpretation given to measurements of the rate of phosphorylation by ATP, which is twice as fast at pH 6 as it is at pH 7 (Ljungström et al., BBA 769, 220, 1984). (Supported by NSF PCM83-09756 and NIH DK36873).

W-AM-G6 CURRENT-VOLTAGE RELATIONSHIPS OF THE ELECTROGENIC SODIUM PUMP OF SQUID GIANT AXON. Paul De Weer, R.F. Rakowski, and David C. Gadsby. Marine Biological Laboratory, Woods Hole, MA.

We determined the current-voltage (I-V) relationship of the forward-running sodium pump of the giant axon of Loligo pealei, from -100 to +20 mV, as the difference between the I-V curves before (or after) and during exposure to 100 µM dihydrodigitoxigenin (H_2DTG). Membrane current was held within ±5 µA/cm^2 by bathing the axons in artificial seawater containing 75 mM Ca^{2+}, 0.1 µM tetrodotoxin, and 1 mM 3,4-diaminopyridine, and internally dialyzing them with a K-free solution containing 200 mM tetraethylammonium HEPES and 20 mM 3-phenylpropyl-triethylammonium bromide (gift of Dr. Clay M. Armstrong). Longitudinal currents were minimized by two ancillary voltage-clamp circuits which kept the potential of the end-pools equal to that of the center pool separated from them by grease seals. Axons were internally dialyzed with 50 mM ^{22}Na and 5 mM each of ATP, phospho-arginine, and phospho-enol-pyruvate; seawaters contained 10 mM K^+; temperature was 17°C. In Na-free (N-methyl-D-glucamine) seawater, both H_2DTG-sensitive ^{22}Na efflux and H_2DTG-sensitive current were slightly (5-10%) lower at −60 mV than at 0 mV. In 400 mM-Na seawater, both H_2DTG-sensitive current and H_2DTG-sensitive ^{22}Na efflux decreased approximately linearly with hyperpolarization, dropping ca. 25-30% between 0 and -60 mV (extrapolated zero-current potential was -200 mV). Supported by NIH grants NS11223, NS22979, and HL14899; D.C.G. was an Established Fellow of the N.Y.H.A.

W-AM-G7 [Na] DEPENDENCE AND VOLTAGE DEPENDENCE OF Na/K PUMP CURRENT IN SINGLE HEART CELLS. David C. Gadsby & Masakazu Nakao, Rockefeller University, New York, N.Y. 10021.

Wide-tipped pipettes were used to record whole-cell currents, elicited by100-ms voltage-clamp pulses to between -140 and +60 mV, from the holding potential, -40 mV, in guinea-pig ventricular cells, at 36°C. Internal and external solutions were designed to sustain Na/K pump current but block ion channel currents. External [K] was 5.4 mM. Internal [Na] and external [Na] were varied by replacing Na with Cs, or with N-methyl-D-glucamine, respectively. Na/K pump current-voltage (I-V) relationships were determined by subtracting steady current levels measured in the presence of 0.5-2 mM strophanthidin (plus 0.1-0.4% DMSO, which in control experiments had no effect) from those in its absence. With 150 mM $[Na]_o$ and 50 mM $[Na]_i$, the pump I-V relationship is sigmoid in shape, and the steep voltage dependence of pump current between -50 and -100 mV suggests that the rate-limiting step in the pump cycle is voltage-dependent (or follows a rapid voltage-dependent step). At 150 mM $[Na]_o$, lowering $[Na]_i$ reduces pump current and shifts the pump I-V relationship to the right, but the voltage dependence persists. That positive shift is in the same direction as the expected shift of the reversal potential for the pump. At 50 mM $[Na]_i$, lowering $[Na]_o$ shifts the pump I-V relationship to the left, also the direction of the expected reversal potential shift. At zero $[Na]_o$, pump current is only weakly voltage-dependent and lowering $[Na]_i$ then reduces pump current by an approximately voltage-independent scaling factor. The results are consistent with Na translocation being the voltage-dependent step, with a strongly voltage-dependent backward rate constant (governing Na influx) but weakly voltage-dependent forward rate constant, as suggested by recent measurements of transient displacement currents generated by the pump. Supported by grant HL-14899, an E.F. of the N.Y.H.A., and the Irma T. Hirschl Trust.

W-AM-G8 SODIUM-CALCIUM EXCHANGE IN SARCOLEMMAL VESICLES PREPARED FROM PORCINE OR BOVINE AORTIC SMOOTH MUSCLE. R.S. SLAUGHTER, M.L. GARCIA, V.F. KING, & G.J. KACZOROWSKI. Merck Inst. Therp. Res., Rahway, NJ 07065.

Vesicle preparations highly enriched in sarcolemmal membranes were prepared from either porcine or bovine aortic smooth muscle. Membrane fractionation was achieved through differential centrifugation and sucrose density step gradient centrifugation. The sarcolemmal fraction was characterized by the activities of Na-Ca exchange and Ca-ATPase, and by the binding of the dihydropyridine calcium channel blocker PN 200-110, the beta antagonist cyanopindolol, and the Na, K-ATPase inhibitor ouabain. At 15 uM $^{45}Ca^{2+}$, the mean Na-Ca exchange uptake in six preparations was 0.20 $\pm$ 0.13 nmol Ca^{2+} accumulated·mg $protein^{-1}\cdot sec^{-1}$ for the fraction taken at the 8-30% interface of the sucrose density gradient. Specific activity was always significantly less in vesicles at the 30-40% interface but total activity was higher because of greater amounts of protein found in this fraction. The kinetics of three of these preparations were analyzed for Ca^{2+} uptake on Eadie-Hofstee plots and found to have K_m's of 15, 9 and 14 uM Ca^{2+} with V_{max}'s of 3.4, 0.45 and 0.56 nmol Ca^{2+} accummulated·mg $protein^{-1}\cdot sec^{-1}$, respectively. The K_m for Na^+-dependent $^{45}Ca^{2+}$ efflux was 5 mM Na^+ and the V_{max} was 2.5 nmol $^{45}Ca^{2+}$ released·mg $protein^{-1}\cdot sec^{-1}$. Thus, the V_{max}'s for uptake and efflux are of comparable values which is consistent with the symmetric kinetic activity previously reported for heart Na-Ca exchange. The K_m's for Ca^{2+} and Na^+ are also well within the range measured in heart but the V_{max} is ca. 10-fold lower than in cardiac membranes. Aortic sarcolemmal Ca-ATPase measured under saturating conditions by ATP-dependent $^{45}Ca^{2+}$ uptake was found to be 5-fold less than the V_{max} for Na-Ca exchange in respective preparations.

W-AM-G9 **$[Ca^{++}]_i$ REQUIREMENT FOR THE OUTWARD MEMBRANE CURRENT ASSOCIATED WITH THE REVERSAL OF THE Na/Ca EXCHANGE.** R. DiPolo, C. Caputo and F. Bezanilla. *Instituto Venezolano de Investigaciones Cientificas, Caracas, Venezuela and Department of Physiology, UCLA, Los Angeles, CA 90024.*

We have previously reported the measurement of a $[Na]_o$-dependent, $[Ca]_i$-activated membrane current in intracellularly dialyzed squid axons under voltage clamp conditions (Caputo et al. 1986, Biophys. J. **49**:232a). Further characterization of this current, under improved clamp conditions, is reported here. In the present experiments, two additional voltage clamp systems were used to clamp the external guard plates to a value that prevented the establishment of a potential difference between the central and lateral chamber compartments. This improvement reduces to a minimum the contribution of membrane currents generated at the axon ends to the current measured in the voltage controlled central pool. Typically the membrane resistance was larger than 15 Kohm cm^2. In most experiments the solutions were (in mM): external: $NaNO_3$, 200 or 0; $Ca(NO_3)_2$, 10; $Mg(NO_3)_2$, 50; TEA-aspartate, 20; NMG-NO_3 (N-methylglucamine), 220 or 420; TRIS-MOPS, 10; pH= 7.8; internal: Na-aspartate, 200 or 20; TEA-aspartate, 100; TRIS-MOPS, 20; $Mg(NO_3)_2$, 5; TRIS-EGTA, 1; NMG-aspartate, variable; pH= 7.3; osmolality= 1000 mOsm. In the presence of 20 mM $[Na^+]_i$ and 200 mM $[Na^+]_o$, the addition of excess $[Ca^{++}]_i$ induced an inward current of 807 nA/cm^2 (n=4, membrane potential=-10 to -20 mV). When $[Na^+]_i$ was 200 mM and $[Na^+]_o$ was 0 mM, the addition of $[Ca^{++}]_i$ induced an outward current of 345 nA/cm^2 (n=5, membrane potential=-10 to -20 mV). The current was greatly reduced when the sodium gradient was abolished. These results are the electrical demonstration of the catalytic effect of $[Ca^{++}]_i$ on the reverse mode of operation of the Na/Ca exchange. Supported by USPHS grant GM30376, The Muscular Distrophy Association of America, NSF-CONICIT (S1-1556) joint program and Fundacion Polar (C.C).

W-AM-G10 IN SQUID AXONS, ATP MODULATES Na/Ca EXCHANGE BY A Ca_i -DEPENDENT PHOSPHORYLATION.
Reinaldo DiPolo and *Luis Beaugé. Centro de Biofísica y Bioquímica. IVIC, Apartado 21827, Caracas 1020A. Venezuela.* Instituto de Investigaciones Médicas. M. y M. Ferreira., Casilla 389, 5000 Cordoba. Argentina.
Phosphorylation is an important cellular regulatory mechanism which has been implicated in the modulation of Ca movements across cell membranes including Ca channels and Ca pumping ATPase. In squid axons ATP has been shown to stimulate the forward (R. DiPolo. J.G. P. 64:503, 1974) and reverse (R. DiPolo. J.G. P. 73:91, 1979) Na/Ca exchange. Whether ATP activates the exchanger allosterically or is hydrolyzed during activation, is still something of a puzzle. The hypothesis that ATP modulates the Na/Ca exchange through phosphorylation has been tested by means of [γ-thio]ATP, an analog of ATP that can act as a substrate for kinases but not for ATPases. Steady state Ca efflux was measured in squid axons dialyzed without ATP, and containing either 0.7 or 100 μM Ca_i. Addition of 1 mM ATPγS drastically increases the Na_o -dependent component of the Ca efflux. The activation by ATPγS: 1-requires the presence of Mg_i, 2-is partially reversible upon removing the analog, 3-is greater than that caused by normal ATP and 4-only activates the exchange system since no effect on the uncoupled Ca efflux (Ca pump) was observed. ^{22}Na experiments were used to monitor the Ca_o -dependent Na efflux (reverse Na/Ca). Without Ca_i and ATP, Na efflux is very small (leak). 1mM ATPγS does not activate the efflux of Na in the absence of Ca_i. In the presence of Ca_i (micromolar) the analog stimulates the Ca_o -dependent Na efflux. Interestingly, neither the Na pump, Ca_i-independent Na/Na exchange, Na_i/Mg_i exchange or Na-K-Cl cotransport are affected by the ATP analog. The experiments indicate that a Ca_i -dependent phosphorylation occurs during the activation of Na/Ca exchange by ATP. (Supported by CONICIT S1-1144, NSF 8500595 and Fundación Polar).

W-AM-G11 MECHANISM OF THE DEPOLARIZING ACTION OF PALYTOXIN ON AXONAL MEMBRANES.
Chau H. Wu and Ken Marx. Department of Pharmacology, Northwestern University Medical School, 303 East Chicago Avenue, Chicago, IL 60611.

Palytoxin (PTX) is a highly toxic substance isolated from marine coelenterates of the genus Palythoa. It causes depolarization of excitable cells, contractions of muscles, and lysis of erythrocytes. Recent studies have shown that in the presence of ouabain the contractile and lytic effects of PTX are inhibited and that PTX inhibits the enzymatic activity of Na,K-ATPase with nearly equal potency to that of ouabain. However, it has not been determined whether the depolarization is due to its action on the sodium pump. We therefore examined the effect of ouabain and other pharmacological agents on the depolarizing action of PTX on crayfish giant axons. At 1 μM concentration, PTX caused a 50-mV depolarization of the axon. The depolarization was inhibited by ouabain or Co^{++} in a dose-dependent manner. Simultaneous application of 2 μM ouabain with either 3 mM Co^{++} or 1 mM La^{3+} completely inhibited the PTX action. Neither tetrodotoxin (300 nM) nor nifedipine (10 μM) antagonized the PTX action. The results are consistent with the hypothesis that PTX binds to Na,K-ATPase and converts the pump into an ionophore with Ca^{++} promoting the conversion.